Design and construction of a mobile equipment for thermal response test in borehole heat exchangers

Anthony Kamarad

Master of Science Thesis EGI-2012-054MSC		
Design and construction of a mobile equipment for thermal response test in borehole heat exchangers		
Anthony Kamarad		
Approved 26/07/2012	Examiner Björn Palm	Supervisor José Acuña
	Commissioner	Contact person

Abstract

In 2010, the Ground Source Heat Pumps (GSHPs) market in the European Union went up over one million (1 014 436 units at the end of 2010 according to EUROBSERV'ER 2011). In 2011, it was estimated around 1.25 million according to Bayer et al. (2012). With more than 378 000 units installed in 2010, according to the Swedish heat pump association (SVEP), the Swedish GSHPs market was the first in the EU. As for the French GSHPs market, it was estimated to 151 938 units in service in 2010, which propelled France at the third rank in the EU. However, despite a relatively important number of GSHPs installed in the whole EU, since 2008 GSHP sales have shrank. Even Sweden which has been the most competitive country sees its GSHP sales decline in the first quarter of 2012 (EUROBSERV'ER 2011).

This report is the achievement of my Master of Science Thesis project. It also represents the end of my studies at INSA Lyon in France and concludes my degree in Energetic and Environment Engineering. This report deals with the improvement of a heat injection apparatus which is available at KTH (Royal Institute of Technology). This equipment is better known as Thermal Response Test (TRT) apparatus. This kind of equipment improves Borehole Heat Exchangers (BHE) design in terms of size and cost benefits. This technology is generally used to design GSHP installations in both domestic and industrial purposes. It allows to determine really important thermal BHE parameters: the *thermal conductivity* of the ground and the *borehole thermal resistance*. The report covers a theoretical description of TRT experiments, the reasons and objectives of such a project, the apparatus design and its construction. The last part is dedicated to a first experimental laboratory results and some problems met during the project course.

Keywords: Thermal Response Test, Borehole Heat Exchanger, Ground Source Heat Pump.

Résumé

En 2010, le marché des pompes à chaleur géothermique (PACg) au sein de l'union européenne s'élevait à plus d'un million d'installations (1014436 unités fin 2010 selon EUROBSERV'ER 2011). En 2011, on l'estimait même à près de 1,25 million selon Bayer et al. (2012). Avec plus de 37800 unités installées en 2010, selon l'association suédoise des pompes à chaleur (SVEP), le marché suédois des PACg était le premier de l'UE. Le marché français était quant à lui estimé à 151 938 d'installations en service en 2010, ce qui le positionnait à la troisième place européenne. Cependant, malgré des chiffres encourageants pour l'union européenne, depuis 2008 les ventes de PACg reculent. Même la Suède qui a pourtant maintenu une forte croissance de son marché durant la dernière décennie, a subi une baisse des ventes des PACg au premier trimestre 2012 (EUROBSERV'ER 2011).

Ce rapport est l'aboutissement de mon projet de fin d'étude effectué au sein de la division « Thermodynamique appliquée et refroidissement », raccrochée au département « Energie et Technologie » de l'université de KTH à Stockholm. Il conclut mes cinq années d'études dans les domaines de l'Energie et l'Environnement effectuées à l'école d'ingénieurs de l'INSA de Lyon (France). Ce rapport traite de l'amélioration d'un appareil réalisé dans les laboratoires de KTH, capable d'injecter une puissance (thermique) dans le sol. Il est généralement connu sous le nom d'équipement pour effectuer des « tests par réponse thermique » (TRT). Ce genre d'appareil est utilisé dans le but d'améliorer le design des sondes géothermiques en termes de dimension et de couts. On a généralement recourt à cette technologie dans le cadre d'installations de pompe à chaleur géothermique aussi bien domestiques qu'industrielles. En effet, cette technologie permet d'évaluer deux caractéristiques thermiques propres à tout site géothermique: la *conductivité thermique* du sol et la *résistance thermique des sondes*. Le rapport inclut une description théorique du principe des tests par réponse thermique, les raisons et les objectifs de ce projet, le design et la construction de cet appareil, et enfin un aperçu des premiers résultats expérimentaux en laboratoire, ainsi que des problèmes rencontrés au cours de ce projet.

<u>Mots clefs:</u> Test par réponse thermique, Sondes géothermiques, Pompes A Chaleur géothermiques.

Acknowledgments

Abbreviations

BHE...	Borehole Heat Exchanger
COP...	Coefficient Of Performance [-]
DAQ...	Data Acquisition
DTDR...	Distributed Thermal Response Test
DTS...	Distributed Temperature Sensing
EER...	Energy Efficiency Ratio [-]
FDM...	Finite Difference Method
GHE...	Ground Heat Exchanger
GSHP...	Ground Source Heat Pump
IEA...	International Energy Agency
TRT...	Thermal Response Test
UPS...	Uninterruptible Power Supply

Nomenclature

a...	Thermal diffusivity [m^2/s]
A...	Cross sectional area [m^2]
c_p...	Specific heat capacity [J/kg K]
D...	Borehole pipe or pipe diameter [m]
D_h...	Hydraulic diameter [m]
E_1...	Exponential integral
$\dot{E}_{pump}$...	Pumping power [W]
f...	Friction factor [-]
G...	Cylindrical source function
J_0, J_1, Y_0, Y_1...	Bessel functions
k...	Slope
L...	Borehole or pipe length [m]
m...	Ordinate at the origin
P...	Wetted perimeter [m]
q...	Heat transfer rate [W/m]
r...	Radius [m]
r_b...	Borehole radius [m]
r_0...	References radius [m]
R_b...	Borehole thermal resistance [K m/W]
R_{rock}...	Rock thermal resistance [K m/W]
R_T...	Total ground thermal resistance [K m/W]
Re...	Reynolds number [-]
t...	Time [s]
T_{bw}...	Borehole wall temperature [°C]
T_f...	Secondary fluid mean temperature [°C]
T_0...	Undisturbed ground temperature [ºC]
$\dot{V}$...	Volumetric flow rate [m^3/s]
w...	Velocity [m/s]

γ...	Euler's constant (= 0.5772...) [-]
ΔP...	Pressure drop [Pa]
ΔP_f...	Pressure drop due to friction [Pa]
η_{pump}...	Pump efficiency [-]
ν...	Kinematic viscosity [m²/s]
λ...	Thermal conductivity [W/m K]
λ_{rock}...	Ground thermal conductivity [W/m K]
ρ...	Density [kg/m³]

Table of content

Index of Figures

Index of Tables

1. Introduction

1.1. Ground Source Heat Pumps

Nowadays, heating and cooling in individual or larger buildings represent 42% of the European energy consumption. For this reason, the use of renewable energies like Ground Source Heat Pumps became a necessity to reduce financial costs and earth degradation.

The GSHP technology is proved and well established. GSHP technology is based on thermodynamic processes and the energy storage under the earth surface. Thermal exchanges occur inside the heat pump due to the change of state of a refrigerant fluid at pressure variations. A heat pump can be described in four key events: evaporation, compression, condensation and expansion of the refrigerant fluid (*Figure 1*). This compression cycle allows the transport and the conversion of the heat to a higher temperature level. The evaporator is connected to the ground loop. For a heating demand, the heat is absorbed by the refrigerant fluid from the secondary fluid (heat carrier fluid) coming from the Ground Heat Exchanger (GHE) pipes. Then, the heat is released inside the heating area via the condenser. In both evaporator and condenser, the refrigerant fluid works under saturated conditions. In the case of a cooling demand, the heat pump has to be reversible and the heat is now absorbed by the secondary fluid and re-injected into the ground via the GHEs.
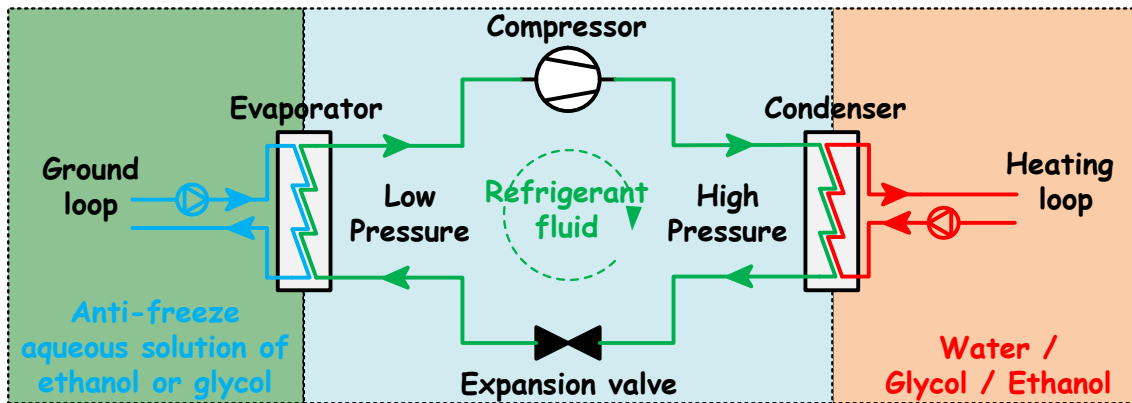
Figure 1: GSHP basic schematic

GHEs are mainly installed into vertical wells (BHE) but sometime also into horizontal, spiral or combined wells. The secondary fluid that circulates through the pipes of the GHE, is an anti-freeze aqueous solution of ethanol or glycol.

The thermal performance: it is the ratio between the output power (heating or cooling) and the external power supply required for running the whole GSHP system. It is commonly known as the Coefficient Of Performance (COP) or the Energy Efficiency Ratio (EER), respectively for the production of heat and cool.

$$\text{COP} = \frac{\dot{Q}_{1h}(\text{energy delivered by the GSHP system for heating application})}{\dot{E}_{compressor} + \dot{E}_{pumps}} \quad (1)$$

$$\text{EER} = \frac{\dot{Q}_{1c}(\text{energy extract by the GSHP system from cooling space})}{\dot{E}_{compressor} + \dot{E}_{pumps}} \quad (2)$$

So, the greatest the external power supply is, the lowest the efficiency of the system will be. A balance between the output and input energies is required to get a good COP or EER. Generally between 3 to 5, the thermal performance is a very useful indicator for comparing heat pump systems.

1.2. Thermal Resistance and Thermal conductivity

In the case of GSHP systems coupled to vertical boreholes, the thermal performance depends on several parameters: the heat pump efficiency, the distribution system inside the building, and the BHE design. This report will focus on BHE design. Indeed, for BHEs, the depth is a decisive parameter for optimizing performances and reducing costs. However, in order to determine the optimal depth of such wells, the heat transfer capacities of both, borehole and ground, have to be known. It refers to the thermal resistance of the borehole heat exchanger (R_b) and the thermal conductivity of the ground (λ).

The total ground thermal resistance (R_T) can be defined as the sum of the rock thermal resistance (R_{rock}) and the borehole thermal resistance (R_b), respectively the resistance of the ground surrounding the borehole wall and the resistance between the secondary fluid in the borehole pipes and the borehole wall.

$$R_T = R_{rock} + R_b \ [\text{K m/W}] \quad (3)$$

The resistance equation (3) is determined between two points, respectively at the secondary fluid mean temperature and the undisturbed ground temperature.

The borehole thermal resistance is divided in three parts: the secondary fluid (R_f), the BHE pipe (R_{pipe}) and the filling material (R_{fm}) (*Figure 2*).
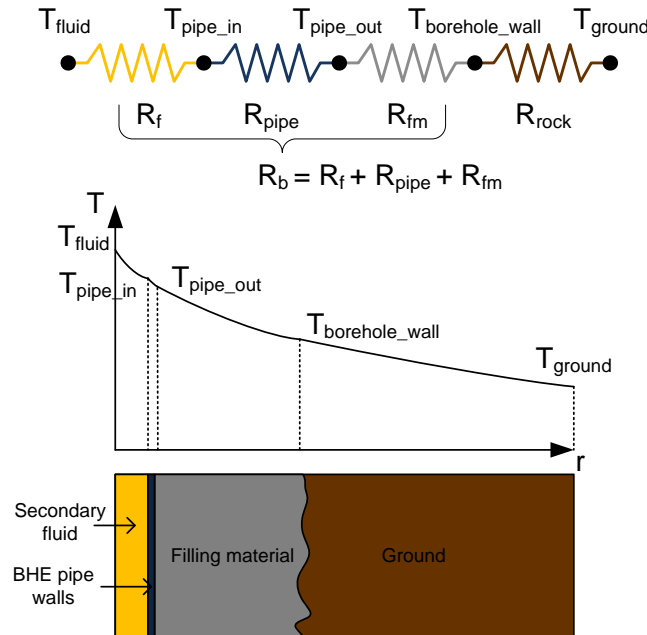
Figure 2: Thermal resistances in BHE

However, to be more accurate, a contact thermal resistance could be added between the BHE pipes and the filling material or between this last and the borehole wall. Moreover, in groundwater filled borehole (instead of concrete for instance) the natural convection can be also another parameter that influences the borehole thermal resistance.

After the combination and simplification, the borehole thermal resistance can also be expressed by the result of the division of the temperature difference (between the mean secondary fluid temperature and the borehole wall temperature) and the heat transfer rate q' [W/m].

$$R_b = \frac{(T_f - T_{bw})}{q} \text{ [K m/W]} \quad (4)$$

So, a smaller borehole thermal resistance is means a better BHE design.

The behavior of a material during a heat transfer is characterized by its thermal conductivity and its geometry. For BHEs, the ground thermal conductivity refers to the transfer capacity of the rock surrounding the borehole walls to transport heat, respectively for cooling and heating demands. This parameter is not easy to determine because of the structures and materials of the ground at different depths (sand, gravel, or rocks), the possible fractures in bedrocks and groundwater flows (leading to natural convection). However, in a steady state, the rock thermal resistance can be estimated as a function of the ground thermal conductivity, and the ratio of the radius at the undisturbed ground condition (r_g) and the borehole radius (r_b). The ground is considered as radial system with the following equation:

$$R_{rock} = \frac{\ln(r_g/r_b)}{\lambda_{rock}} \text{ [K m/W]} \quad (5)$$

1.3. Thermal Response Test

1.3.1.   Basics & Operation

As stated previously, an optimal Borehole Heat Exchanger design requires knowledge of the heat transfer capacities of both borehole and ground, with a certain accuracy. The ground thermal conductivity and borehole thermal resistance can be determined via laboratory or/and field measurement on real borehole exploitation sites. However, due to multiple parameters that influence the properties along the borehole length and its surroundings (structure, materials, bedrock fissures, groundwater, and borehole deviation), it is more suitable to carry out an in situ measurement to get better approximation. Thermal Response Test is the most developed technology for it.

The idea of a Thermal Response Test is to inject or extract heat from the ground as a heat pump does. In that case, the goal is not to heat or cool a place, but to obtain information about the temperature behavior in and around a specific BHEs installation. For instance, a quick change of the temperature represents a high ground thermal resistance (low thermal conductivity).

TRT consist of circulating a heat carrier fluid through BHEs coupled with a constant heat power injection or extraction, for a certain period of time (this report will cover only the

injection part). This procedure allows the acquisition of the fluid temperature over the time. Thanks to analytical models (presented section 1.3.3), and under appropriate conditions (period of time relatively long), a good estimation of the ground thermal conductivity and borehole thermal resistance can be made.

A TRT apparatus can be simplified (see *Figure 3*). It can be split into three categories. First, the working devices. It includes an electric heater and a pump. Those two are used to generate the heating power which will be injected into the borehole. Then, the measuring devices for the data acquisition (a flow meter and an inlet and outlet borehole temperature sensors). Those allow to determine the real injected heat and follow the temperature changes over the time. Finally, the last category refers to starting and functional components. It gathers valves, to open, close or drain the equipment; an open tank to remove air from the system and to fill it with the circulating fluid; and quick connections to the borehole pipes.
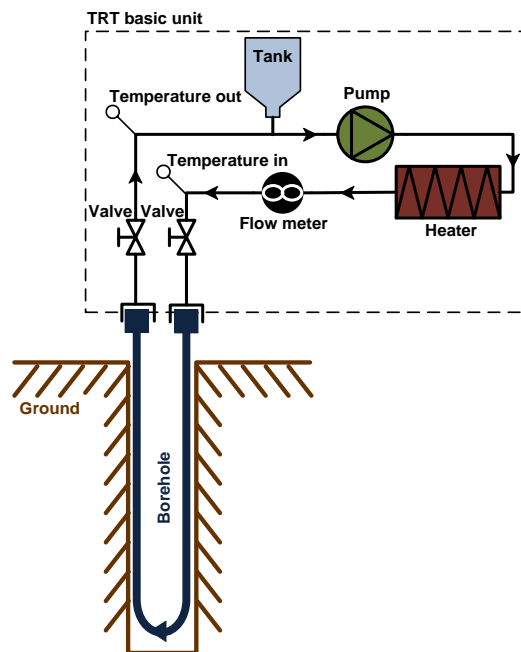
Figure 3: Schematic view of a standard TRT equipment

Even though the construction of TRT apparatus does not seem to be so complicated, some conditions and extra recommendation have to be respected, according to the "Guidelines for thermal response testing" developed by the working group of Annex 13 "wells and boreholes" of the Implementing Agreement on Energy Conservation through Energy Storage of the International Energy Agency (IEA) (further information on http://www.thermalresponsetest.org/). In terms of equipment, the heater has to be able to supply a steady heat load and to allow several thermal load steps. The flow rate should be adjustable via the circulating pump. Safety devices should be installed to control pressure, fluid leakage, and/or over-heating. To minimize the influence of ambient temperature variations, all devices and pipes have to be thermally isolated, and connection pipes have to be as shorter as possible to avoid load fluctuation when running the system. On the other hand, during the operation of the system, air has to be removed from the circulating fluid, and inside the borehole. The flow should normally to be turbulent during the entire measurement.

In order to explain how a Thermal Response Test operation is set up, an illustration of temperature behavior over the time is presented *Figure 4*. The borehole incoming and outgoing temperatures, respectively the red and blue dots on the graph, are plotted over time during the different test phases (the yellow ones are the mean temperature, used for analysis).
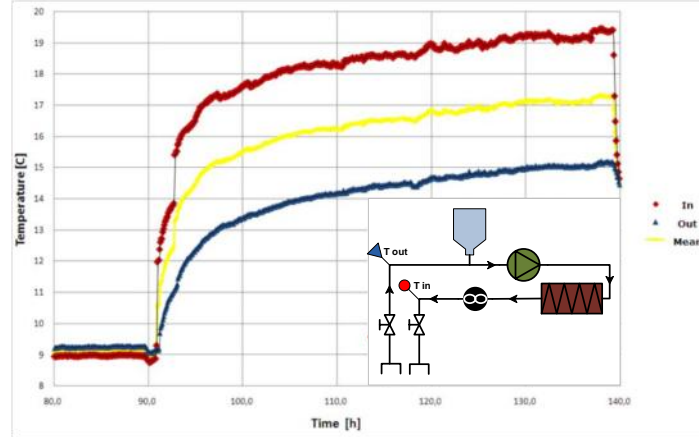
Figure 4: Recording temperature profiles (Acuña J. 2010)

Two distinct steps can be distinguished. During the first one, no heat injection is made. The fluid circulates only in view to determine the undisturbed ground average temperature. For this reason, both temperatures are the same. This phase is commonly known as the "pre-circulation period". Then, the heat injection starts. Both temperatures increase until there is a constant temperature difference.

1.3.2.   State of the art

Even if the theory behind the analysis of TRT exists since many years, according to Sanner et al. (2005), the first development of a theoretical technique of TRT dates from 1976, and was published by Choudary. Mogensen (1983), Claesson et al (1985), Claesson and Eskilson (1988), and Hellström (1991) have continued to work on this topic. Palne Mogensen was the first to develop a thermal response tester (June 1983). With the help of two students from KTH (Royal Institute of Technology, Sweden) they built a chiller system with R22 as refrigerant. The system provided a constant cooling effect of 2.7 kW. The condenser side was cooled with water, while the evaporator side was connected to the incoming and outgoing secondary fluid lines of the borehole. A circulation pump and PT100 temperature sensors were also included in the system (see *Figure 5*).

Figure 5: The first thermal response tester (Acuña J. 2008)

In 1997, Hellström undertook the first practical tests on a real borehole heat storage. In 1995, a test mobile equipment was built. It was developed by Luleå technical University (Eklöf and Gehlin 1996). Subsequently, some similar developments followed almost simultaneously in the United State, and later in Germany and Netherlands. The particularity of the last rig (from Netherlands) is that it uses a heat pump instead of an electric resistance heater. This type of rig requires more control and equipment. Nowadays, with the ground storage application growth, the use of test equipments increases. In 2000, more than 30 countries around the world used the TRT technology.

A new technology known as Distributed Temperature Sensing (DTS) has recently been coupled to the conventional Thermal Response Test. With this technology, the circulating fluid temperature can be measured at different depths via optic fiber cables. This allows to determine thermal properties at different levels of the borehole and get a thermal profile more precise. This combination of those two technologies is known as Distributed Thermal Response Test (DTRT) and it has been applied to U-pipe BHE in (Acuña J. 2010) and to coaxial BHEs in (Acuña et al, 2012) and (Acuña & Palm, 2012).

1.3.3.   TRT Theory

1.3.3.1.   Background

The theory behind the design of ground heat exchangers, has been developed by Ingersoll et al. in 1948, through the line source model. Then, Carslaw and Jaeger (1959) used the assumption of a constant heat injection to simplify this theory. So, this approximation of the mathematical expression of the temperature in a BHE (equation (6)) became the starting point for most Thermal Response Test analysis.

$$T(r,t) = \frac{q}{4\pi\lambda} \int_{\frac{r^2}{4at}}^{\infty} \frac{e^{-u}}{u} du = \frac{q}{4\pi\lambda} E_1\left(\frac{r^2}{4at}\right) \quad (6)$$

The cylender source model is another mathematical model developped by Ingersoll et al. (1948) presented in the equations (7), (8) and (9). Indeed, the line source is no more or less than a simplification of the cylinder source model. In the cylinder source model, the BHE is considered as an infinite cylinder instead of an infinite line.

$$T(r,t) = \frac{q}{\lambda} G(z,p) \quad (7);$$

$$G(z,p) = \frac{1}{\pi^2} \int_0^{\infty} f(\beta) d\beta \quad (8); \quad f(\beta) = \left(e^{-\beta^2 z} - 1\right) . \frac{[J_0(p\beta)Y_1(\beta) - Y_0(p\beta)J_1(p\beta)]}{\beta^2 [J_1^2(\beta) + Y_1^2(\beta)]} \quad (9)$$

$G(z,p)$ is the cylindrical source function, and J_0, J_1, Y_0, Y_1 are Bessel functions of the first and second kind.

More recently, numerical models are used. Since Berberich et al. (1994), different models (one or two dimensional finite model), ground thermal parameter estimations, BHE geometry assumptions, and other improvements have been developed and combined to design borehole heat exchangers.

1.3.3.2. Line source model analysis

In this section, the line source model description refers to Monzó P. (2011). First of all, it is important to highlight that the line source model, as well as the cylinder line model and numerical models, are based on several assumptions:

➢ In the ground, conductive heat transfer is only considered (convection is neglected).
➢ Thermal process is symmetric and unidirectional (radial direction from the borehole axis).

As it has been previously pointed out, the equation (6) is the starting point for the analytical line source model. However, to make this equation usable, the line source temperature is determined at the borehole radius (r_b). Then, in order to evaluate the expression of the secondary fluid mean temperature (T_f), the borehole thermal resistance (R_b) has to be taken into account (see equations (4.bis) and (10) proposed by Mogensen, 1983).

$$T_f(t) = T_{bw}(t) + q.R_b \quad (4.bis)$$

$$T_f(t) = \frac{q}{4\pi\lambda_{rock}} E_1\left(\frac{r_b^2}{4at}\right) + q.R_b + T_0 \quad (10)$$

For a normal borehole (cylindrical heat injection pipes), Ingersoll and Plass (1948) have showed that this equation can be used with a less than 2% error if $t > \frac{20r_b^2}{a}$, corresponding to the 10 to 20 hours range.

Plus, E_1 is called exponential integral, and it can be approximated with simple relation for large value of the parameter "at/r²".

$$E_1\left(\frac{r^2}{4at}\right) = \ln\left(\frac{4at}{r^2}\right) - \gamma \quad \text{for} \quad \frac{at}{r^2} \geq 5 \quad (11)$$

γ is the Euler's constant ($\gamma = 0.5772...$). Moreover, the maximum error is 2.5% for values of $\frac{at}{r^2} \geq 20$ and 10% for $\frac{at}{r^2} \geq 5$.

So, according to the equation (11), the secondary fluid mean temperature equation can be expressed as the following equation:

$$T_f(t) = \frac{q}{4\pi\lambda_{rock}}\left(\ln\left(\frac{4at}{r_b^2}\right) - \gamma\right) + q.R_b + T_0 \quad (12)$$

Regarding the equation (12), the secondary fluid mean temperature depends only on the natural log of time. The equation (12) can be thus estimated with a simple linear equation:

$$T_f(t) = k.\ln t + m \quad (13) \quad ; \quad k = \frac{q}{4\pi\lambda_{rock}} \quad (14)$$

$$m = q.\left[R_b + \frac{1}{4\pi\lambda_{rock}}\left(\ln\left(\frac{4a}{r_b^2}\right) - \gamma\right)\right] + T_0 \quad (15)$$

k is the slope of the curve and m the ordinate at the origin.

Before going any further, it is necessary to reemphasize that all those equations are correct only if the heat injection is constant. So, respecting this criterion, the ground thermal conductivity, related to k, can be determined with the equation (16).

$$\lambda_{\text{rock}} = \frac{q}{4\pi k} \quad (16)$$

Regarding the borehole thermal resistance, two ways exist to get its value once the ground thermal conductivity has been determined. Indeed, the borehole thermal resistance can be constant or dependent on the time, see equation (17) and (18) respectively.

$$R_b = \frac{m - T_0}{q} - \frac{1}{4\pi\lambda_{\text{rock}}}\left(\ln\left(\frac{4a}{r_b^2}\right) - \gamma\right) \quad (17)$$

$$R_b = \frac{T_f(t) - T_0}{q} - \frac{1}{4\pi\lambda_{\text{rock}}}\left(\ln\left(\frac{4at}{r_b^2}\right) - \gamma\right) \quad (18)$$

a is the thermal diffusivity, defined as: $a = \left.\frac{\lambda}{\rho c_p}\right|_{\text{rock}}$ (ρc_p being the volumetric heat capacity in $\text{J}/(\text{m}^3 \cdot \text{K})$).

In a real case, the power supply is not constant during the test and it is difficult to maintain a constant heat injection during the whole Thermal Response Test (Eklöf and Gehlin, 1996). Consequently, the secondary fluid mean temperature might be considered as the sum of constant heat pulse contributions at a certain time interval according to Eskilson (1987) and Hellström (1991). This step-analysis is described below:

$$\Delta T(q_1, q_2, \dots, q_n) \equiv \Delta T(q_1) + \Delta T(q_2) + \cdots + \Delta T(q_n) \quad (19)$$

$$q(t) = \begin{cases} q_0 = 0 & t < t_1; \ t_1 = 0 \\ q_1 & t_1 < t < t_2 \\ q_2 & t_2 < t < t_3 \\ & \cdots \\ q_n & t_{n-1} < t < t_n \end{cases} \quad (20)$$

As aforementioned, this analysis is based on the principle of super positioning. In this configuration, the mean secondary fluid temperature expression is:

$$T_f(t) = \frac{q_{\text{ref}}}{4\pi\lambda_{\text{rock}}}\tau_N(t) + \left[q_N\left(\frac{1}{4\pi\lambda_{\text{rock}}}\left(\ln\left(\frac{4a}{r_0^2}\right) - \gamma\right) + R_b\right) + T_0\right] \quad (21)$$

$$\tau_N(t) = \sum_{n=1}^{N}\frac{q_n - q_{n-1}}{q_{\text{ref}}}\ln(t - t_N) \quad \text{with} \quad q_{\text{ref}} \neq 0 \quad (22)$$

τ_N is a dimensionless parameter, with t the time in the interval $t_n + \frac{r_0^2}{4a} < t < t_{n+1}$.

Due to the linear relation between the secondary fluid mean temperature and τ_N, the slope of this curve (k') allows to determine the ground thermal conductivity as suggested equation (23). Then, the borehole thermal resistance (equation (24)) is estimated using equation (21).

$$\lambda_{\text{rock}} = \frac{q_{\text{ref}}}{4\pi k'} \quad (23)$$

$$R_b = \frac{T_f(t) - \frac{q_{ref}}{4\pi\lambda_{rock}}\tau_N(t) - T_0}{q_N} - \left(\frac{1}{4\pi\lambda_{rock}}\left(\ln\left(\frac{4a}{r_0^2}\right) - \gamma\right)\right) \quad (24)$$

The line source model fit well with the measured temperatures. The ground thermal conductivity and the borehole thermal resistance are close to the reality. The cylinder source method shows values 10% to 15% higher compared to line source estimation, whereas the one-dimensional FDM numerical model gives values 4% lower (Gehlin and Hellström, 2003). These deviations are higher in short time experiment. In increasing time, the estimated parameters tend to match better with the line source model. It is recommended to exclude the first 10 hours of testing to get better estimations, but also to have a minimum of 30 hours of data to converge toward good estimations.

1.4. Objectives

This project has been built in accordance with KTH's expectations and needs and the Thermal Response Test background. It focuses on two main objectives: to stabilize the heat power and to create a friendly remote control system.

➢ It has been theoretically and experimentally proved that the heating power is influenced by the voltage variation in the national grid. This is a key issue to get accurate estimations of ground properties. So, the first goal is to make the power load as steady as possible.

➢ The second goal is to control the TRT system away from the testing site. The heating power and the flow rate have to be modifiable from any internet access, at any time. A remote control and a user interface with a login and password must be created to make the system control and data acquisition friendly.

2. Design and Construction of the TRT apparatus

2.1. The design

Before starting this project, KTH already had a simple TRT apparatus, as presented in section 1.3.1. For this reason, improvements had to be done in terms of control, safety, and data acquisition. The first step has been to point out problems and lacks of this previous equipment. Then, by combining this approach with actual expectations, we defined the requirement specifications for the new TRT apparatus. In *Figure 6* are shown the characteristic blocks of the new TRT apparatus. Each block has a specific function which will be discussed later in this report.
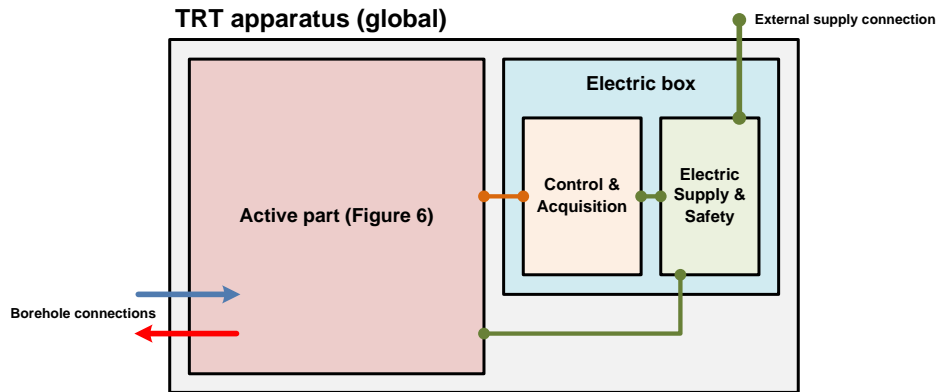
Figure 6: TRT apparatus overview

2.1.1. Active part

The active part groups all components in contact with the secondary fluid (Figure 7). The bold line (with direction arrows) represents the secondary fluid loop when a test is running. Other lines are sensor connections and filling fluid connections.
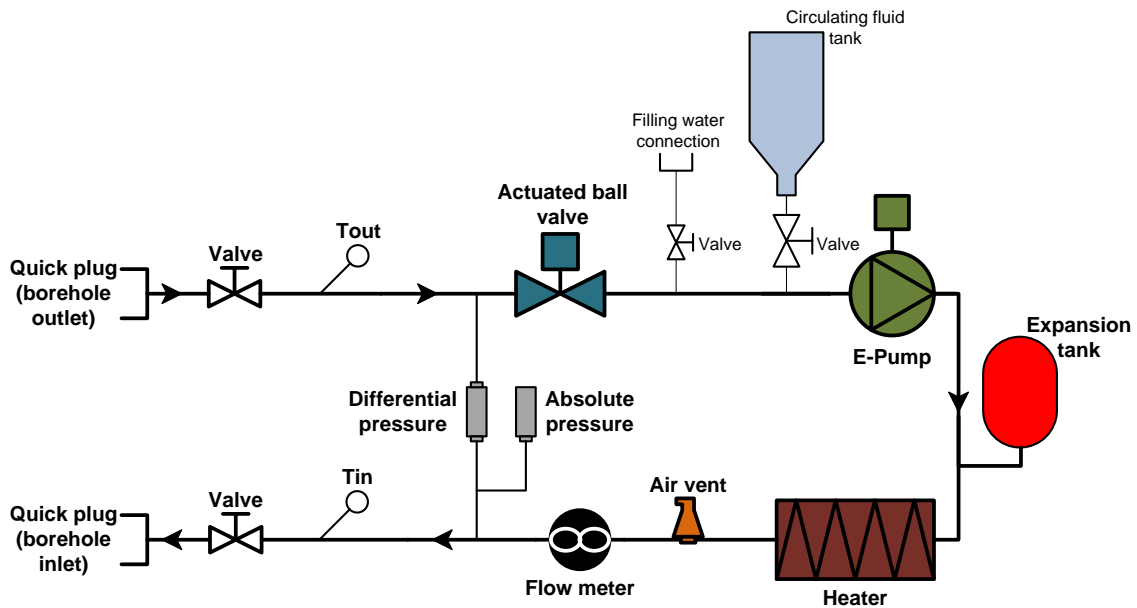
Figure 7: Schematic view of the active part

2.1.1.1. Heat load control

The heat load has been one of the principal concerns of this project. Several researches, technical options, and discussions were needed in order to make the heat injection as constant as possible and to control the power of the eclectic heater.

The electric heater that is used is the same than in the previous TRT apparatus (see "Electric heater" *Table 1*). It is a three phases electric immersion heater with a maximum of 13kW. The output power can be changed to 7-9-11-13 kW in three stages for all outputs or in two stages for 7 and 9kW. The supply is plug to a terminal block and then re-wired to heating resistances and manual switches to start and to set the output power of the heater. Indeed, the power change is made via a manual thermostat 3-pole. However, according to wiring diagram available in the heater's data booklet, an external control unit can be added to set the power. Nevertheless, this unit is not furnished and it is necessary to design a remote control system. Therefore, it has been made regarding the following description.

Still according to the heater's data booklet, before starting the heater, the maximum power has to be fixed and cannot be changed when it is running. *Figure 8* represents the wiring diagram for a maximum of 9kW.
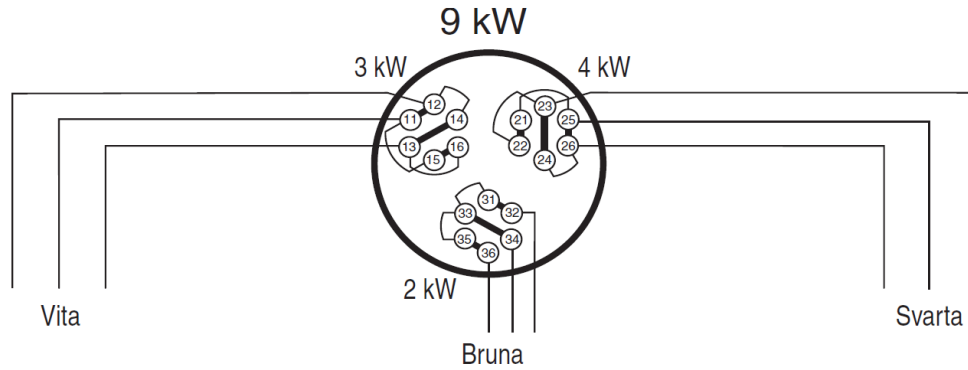
Figure 8: Immerged heating resistances wiring diagram for 9kW

Remark: There is a different wiring diagram for each output power.

Once the maximum output power is chosen, the heat load can be then controlled. It is possible to replace certain bridges in the electrical connections with external contactors. The wanted stages can be set in activating relays in different configurations via an external control unit according to *Figure 9*.
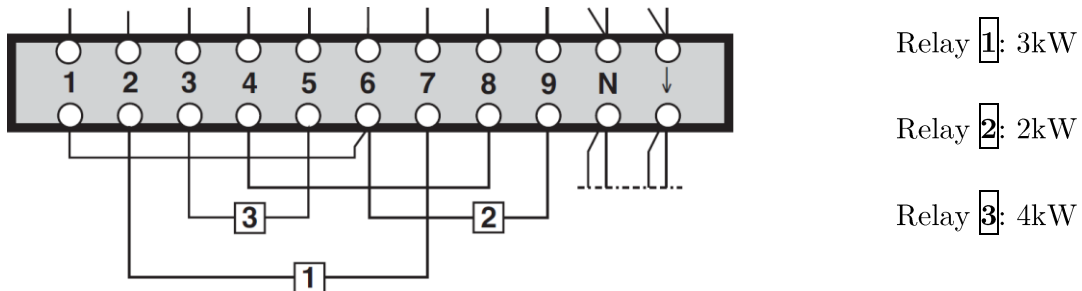
Figure 9: Relay connections diagram for 9kW in three stages

Concerning the stabilization of the power supply, it has been carried out in upstream of the heater. Indeed, several options were possible in order to fix this problem. The two first ideas were to connect the heater to an Uninterruptible Power Supply (UPS) or a voltage stabilizer unit. Both deliver a constant output voltage whatever the grid fluctuations. With the first one, there was possibility to add extra batteries in case of outage. However, for size and incompatibility reasons (dry working area and non mobile units), these solutions have been given up. At the end, a power thyristor unit choice (see "Power stabilizer" *Table 1*) has been the best solution. The power is stabilized in a range from 0 to 13kW depending on an external signal.

So, the electric heater is turn ON and OFF through an external power thyristor unit which also maintains the power supply constant. The heat load is changed via externally controlled relays.

2.1.1.2.   Flow rate control

Another expected improvement was to control the flow rate. The choice of a suitable pump was essential to guarantee the performance and the precision of the new TRT apparatus.

First of all, the characteristics of the pump had to be defined regarding both the turbulent flow consideration and the maximum expected pressure drop in different borehole heat exchanger types. Indeed, it is recommended to run a Thermal Response Test in a complete turbulent condition to get a better heat transfer between the secondary fluid and the inner surface of the borehole pipes. The Reynolds number (Re) allows to analyze the flow state of any moving fluid in pipes. It is a dimensionless number which can be calculated following the equation (25). Depending on the number, there are three types of fluid flow: laminar (Re≤2300), transitional (2300<Re≲4000) or turbulent (Re>4000). Nevertheless, to reach fully turbulent flow conditions, it is necessary to have Re higher than 10000, according to Acuña J. (2010).

$$Re = \frac{w\, D_h}{\nu} \quad (25)$$

Then, according to the regular pressure drop in ducts (equation (26)), the head loss in a tested borehole can be estimated. For this purpose, the friction factor needs also to be estimated as expressed in equation (27) or (28).

$$\Delta P_f = f\, \frac{\rho w^2}{2}\, \frac{L}{D} \quad (26)$$

$$f = \frac{64}{Re} \quad \text{(for Re≤2300)} \quad (27) \quad \text{or} \quad f = \frac{1}{(0.79 \ln Re - 1.64)^2} \quad \text{(for Re>2300)} \quad (28)$$

Estimation of the maximum pump characteristics assuming a borehole length of 300m, pipes of the type PE 40x2.4 mm, ethanol 15 wt-% as secondary fluid at a mean temperature of 20°C, and a flow rate of 1L/s:

$Re = 19171$ (turbulent flow); $\quad D_h = \frac{4A}{P} = D$ (for cylindrical pipes).

f = 0.0264

ΔP_f = 116010 Pa = 1.1601 bar → ΔP_{ftot} = 2.3203 bars.

Remarks:

- The thermophysical properties of aqueous solutions using ethanol are taken from Melinder (2007).
- The singular pressure drop at the bottom part of the borehole (U-form) has not been taken into account as well as pressure drop into the TRT equipment.

So, according to the pump range (*Figure 10*), and the fact that the pumping power is related to the volumetric flow rate and the pressure drop (equation (29)), a low energy consuming pump able to achieve a maximum volumetric flow rate of 1L/s with a head around 3 bars has been chosen.

$$\dot{E}_{pump} = \frac{\Delta P.\dot{V}}{\eta_{pump}} \quad (29)$$
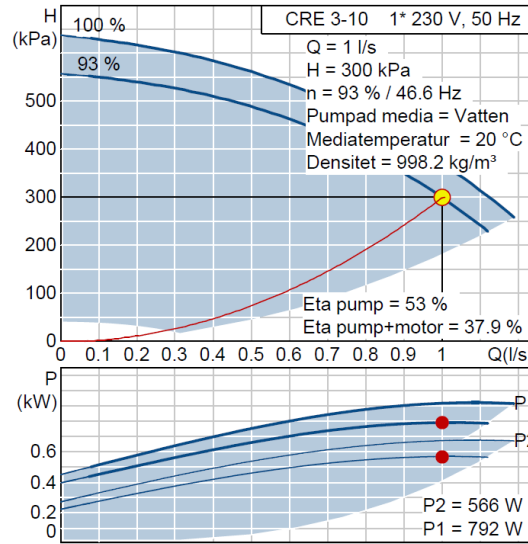
Figure 10: Characteristic curve of the selected pump

Moreover, with a view to satisfy the characteristics above and control the flow rate, this pump integrates an E-motor, i.e. a motor with an internal frequency converter (see Pump" *Table 1*).

2.1.1.3.   Other requirements

This section deals only with well known components. However, it is important to integrate them in the design of a TRT apparatus. They contribute to guarantee a smooth functioning, increase the security and facilitate the use of the system.

The different components can be classified in five categories. Each category gathers components with the same requirement. However, some of them can belong to two categories which link them to one another also (*Figure 11*).
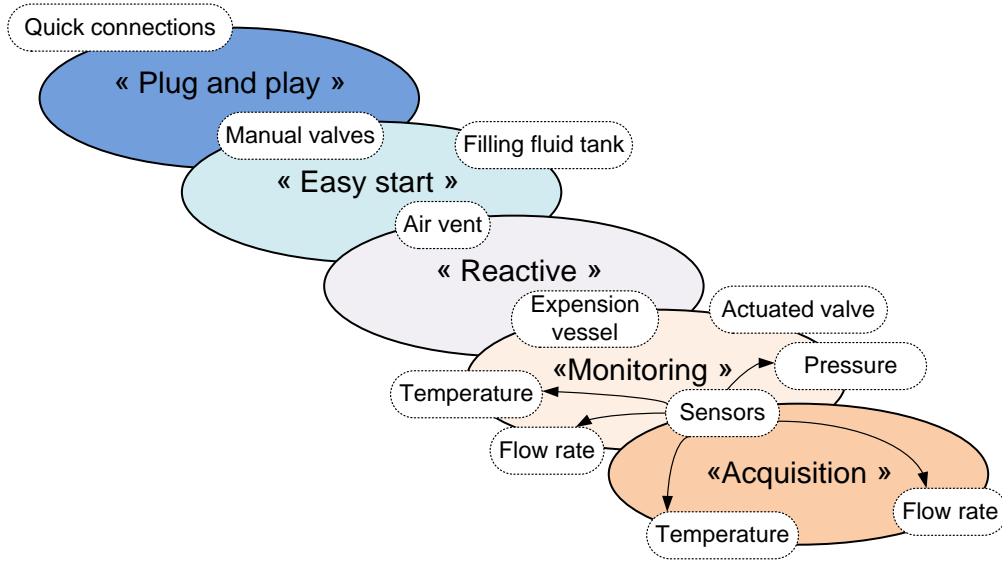
Figure 11: Complementary requirements diagram

Description of the different categories:

- "*Plug and Play*": A Thermal Response Test apparatus must be mobile and fast to install. Therefore, quick connections and manual valves have been installed to facilitate the connection of the system to a real borehole exploitation site.
- "*Easy start*": Before running a test, the whole system must be filled with the circulating secondary fluid. Indeed, the pump and the heater cannot work properly without fluid or if there are bubbles of air. Filling devices (a tank and a secondary connection) and an air vent are so necessary to make the start simple and remove air respectively.
- "*Reactive*": During a test, the system must be able to adapt itself to the change of properties of the fluid. Indeed, with the temperature variations, the fluid properties will change as well as the pressure in the pipes. The system should be able to operate as closed and open system. An expansion vessel is required.
- "*Monitoring*": Since the system is supposed to run during several days without supervision, it must integrate means of control in order to avoid any damage. For instance, the pressure sensors allow to control if the pressure is too high or too low (leakage). Malfunctioning can also be detected with the temperature sensors in case of overheating (temperature two high) or with the flow meter in case of unexpected low flow. An externally controlled valve has been added to close the hydraulic loop in case of important dysfunction.
- "*Acquisition*": This category is related to most of the previous components. Beyond safety purposes, the sensors are used for data acquisition, which will be recorded and used for the analysis of the thermal properties of BHEs.

So, even if all of these components are not working devices like the heater or the pump, their role is essential to meet the new TRT apparatus requirements.

2.1.2.   Electric box

2.1.2.1.   Electric Supply & Safety

It is not useless to remember that most of the components mentioned above are electric devices, especially the pump, the heater and the monitoring and acquisition devices. For this reason, and still according to the requirement to build a "plug and play" apparatus, the electric supply of all these devices is realized from a single socket. This last is connected to the three phases supply available in the testing site. The power is then redistributed through each electrical equipment, depending on their supply voltage type (400V 3P+N, 230VAC or 24VDC). For instance, the 3-phase equipments are directly connected to the general supply, the 230VAC ones to a single phase of the general supply and the 24VDC to a transformer.

Other requirements like "easy start", "reactive" and "safe" have been integrated to the electric part. A general switch has been installed between the general supply and all electrical equipments, to manipulate them before turning on, without having to plug and unplug the power. As mentioned in section Heat load control, a power stabilizer is also used to lower the effect of the grid fluctuation inside the heater. Moreover, since the heater can operate at high power, and that water flows through the system can be in contact with electrical components, fuses and very sensitive circuit breakers have been built in the electrical panel. To complete the safety requirement, the whole electronic components inside and outside the electric box have been connected to the ground.

In addition to the electrical components listed above and the electric devices of the "active part", other electric components which function is different but still important, are presented in the next section.

2.1.2.2.   Control & Data Acquisition

As it has been previously expressed in the project objectives, the second idea is to develop a remote control to operate the system and acquire data. This represents a full-fledged work in the development of the new TRT apparatus. This work is mainly based on electronic and programming issues (see section 2.2 User Interface).

However, to implement such an approach, it is essential to have suitable automation and data acquisition tools. The two basic elements are a DAQ card and appropriate software (as well as a computer to operate both). With these two elements, it is then possible for the user to communicate with the different devices she/he wants to control. An DAQ card which allows to send and receive signals whether analog or digital and LabVIEW® were chosen. To ensure all controls, a specific control unit for the pump and five relays were added to the electric panel. Indeed, the pump is provided with a control unit which allows to control different parameters like the pump speed. The user must also be able to turn on and off the devices such as the pump, the heater and the actuated ball valve. For this reason, a relay is assigned to each one of them to control their activation via an output of the DAQ card. In the case of the heater, the power stabilizer unit replaces the relay but is still controlled via the DAQ card, while the other three relays are used to control the power of the heater.

In term of data acquisition, the electronic part is only made of a computing unit with a display for the flow rate and un-terminated wires for the pressure and temperature sensors. The flow rate value is transmitted to the DAQ card by pulses. Each pulse represents certain among of fluid flowing through the flow meter (unit volume). Regarding to the pressure sensors, they deliver a 0-10V analog signal. This signal is read by the DAQ card and then converted in accordance with the range 0-5bars. The temperature sensors are platinum resistors. The DAQ card was so configured to convert a value of resistance into temperature. The DAQ card has been calibrated in using a conversion table determined with a constant-temperature bath (*Figure 12*).
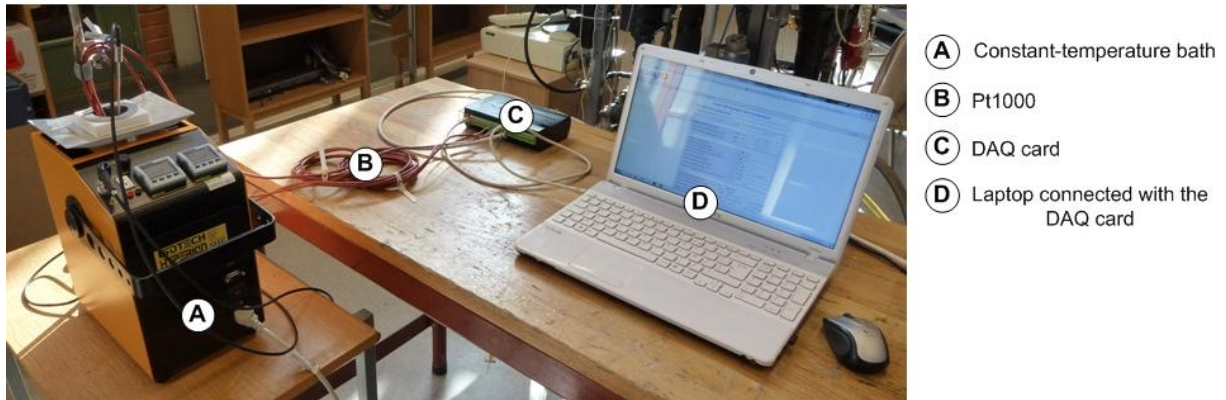
Figure 12: Pt1000 calibration

To conclude with the design, *Figure 13*, *Figure 14* and *Table 1* give a detailed overview of the new TRT apparatus with pictures and a list of the components mentioned above.
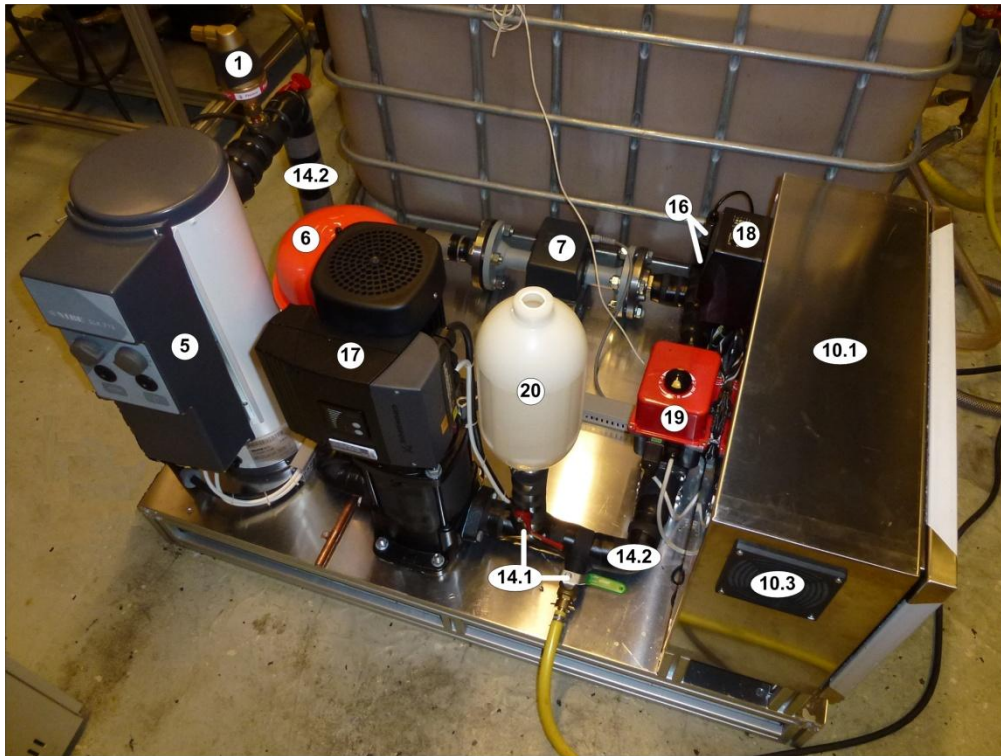
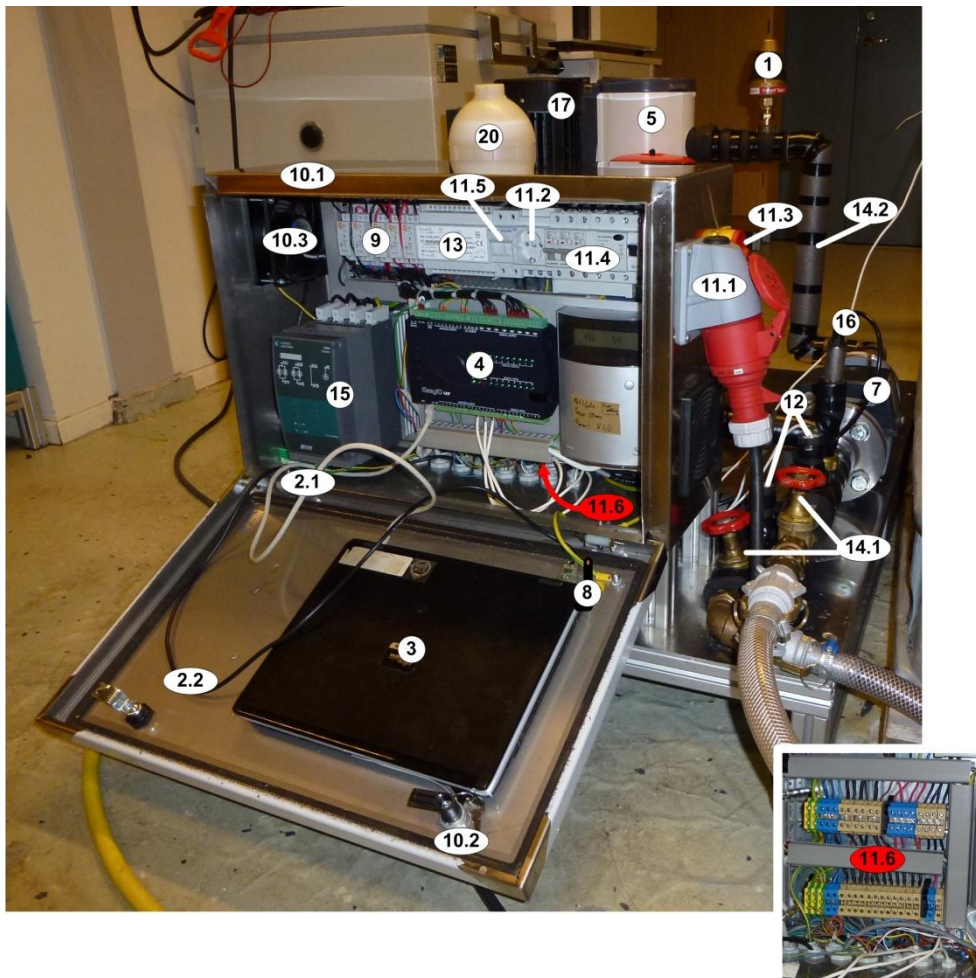Figure 13: Picture of the TRT apparatus (1/2)

Figure 14: Picture of the TRT apparatus (2/2)

17

Table 1: Main and complementary components

Air vent (**1**)	-	Flamco Flexvant® Super ½"
Communication cables (**2**)	- -	Ethernet cable (**2.1**) USB-RS485 converter cable (USB-RS485-WE-5000-BT, FTDI) (**2.2**)
Computer and software (**3**)	- -	Fujitsu Siemens Laptop LabVIEW® 2011 (National Instruments)
DAQ unit (**4**)	-	EasyIO30P IO-30P-ME controller
Electric heater (**5**)	-	NIBE ELK 213 (400 V 3 N AC 50Hz)
Expansion vessel (**6**)	-	Zilmet 1,5L - 5bars
Flow meter (**7**)	-	Brunata HGP-SIV15-40 and HGP15-40-07
Internet access module (**8**)	- -	HUAWEI Mobile Broadband E637. Ventelo
Relays (**9**)	-	MALMBERGS, Switching relay, 10A AC21, 1 changeover, 24V AC/DC (x5)
Electric box (**10**)	- - -	Stainless steel box (**10.1**) Key locker (**10.2**) Fans (**10.3**)
Electric components (**11**)	- - - -	400V 3P+N socket (**11.1**), 230V socket (**11.2**) General rotary switch (**11.3**) Circuit breakers (**11.4**) and fuses (**11.5**) Terminal blocks, cables and wires (**11.6**)
Temperature sensors (**12**)	-	PT1000 (x3)
Transformer (**13**)	-	Noratel DC-Powersupply 0-230/250V to 24VDC 50/60Hz
Pipes and connections (**14**)	- - - -	Copper ducts (DN 28mm main loop) Manual valves (**14.1**) Elbows, reductions and quick plug pipe connectors Polyurethane foam tube and/or insulating flexible tube with cell structure (**14.2**)
Power stabilizer (**15**)	-	Invensys EUROTHERM 7200A Power Thyristor Units
Pressure sensors (**16**)	-	GE UNIK 5000 Absolute pressure gauge (0-5bars) and Differential pressure gauge (0-5bars)
Pump (**17**)	-	Grundfos CRE3-10 A-A-A-E-HQQE
Pump control unit (**18**)	-	Grundfos CIU200-CIM200
Actuated ball valve (**19**)	-	FGinox 316 ROBINET BS PI 3P 1"1/2 FF
Water tank (**20**)	-	NIBE plastic tank

2.2. User Interface

Before describing the user interface and the programming that goes behind, it is important to show the interaction and the hierarchy between the main devices of the TRT apparatus in order to clarify their role, especially in term of measurement and control (see *Figure 15*).
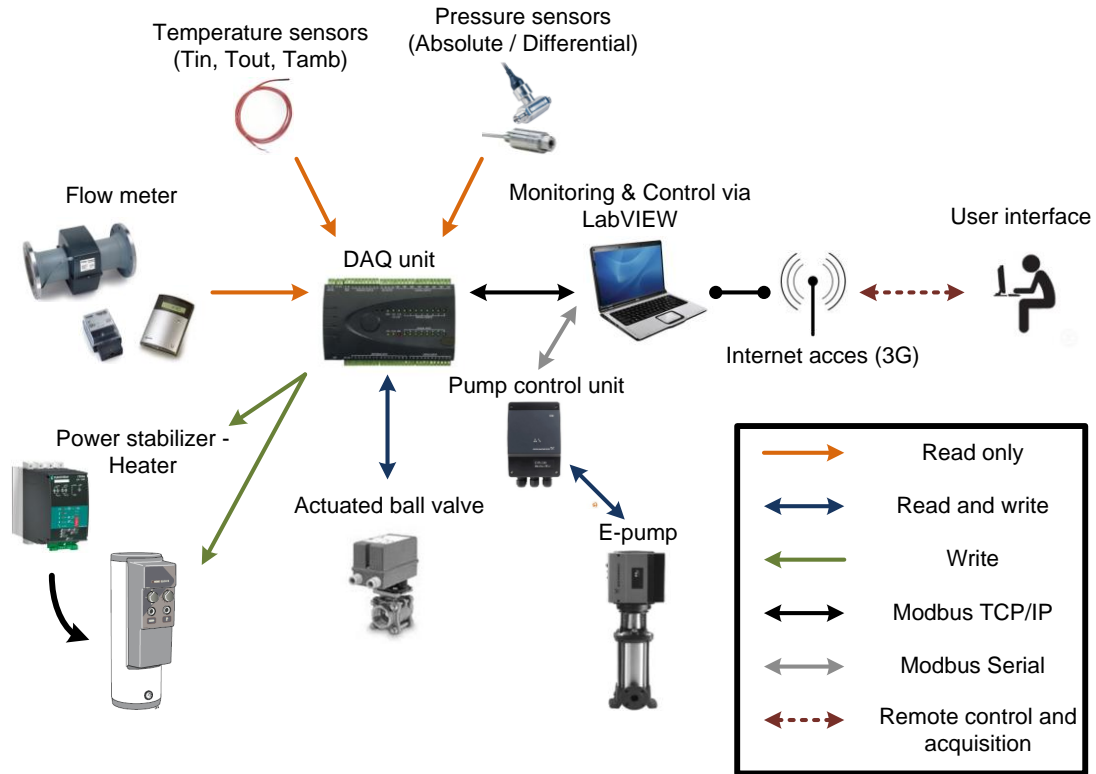
Figure 15: Sketch of the system architecture

The figure above shows that everything starts from the user, therefore the importance of the user interface.

The user interface has a threefold interest. The first objective is to hide the programming code and regulation parts. The second is that the user can operate the system under the wanted conditions, in the easiest ways, at any time and from any internet access. Finally, since the user is not permanently in the testing field, she/he must be alarmed in case emergency. The user needs also to have an overview of the ground behavior and a first approximation of its properties.

The automation and the control of systems require always to write in a programming language. It was necessary to choose a program to automate an installation involving several programmable devices, while integrating an intuitive language. LabVIEW® was chosen because of its scope of practice (control, measurement, instrumentation and automated test from a PC). Its language is also preferred by engineers and researchers often more familiar with experimental protocols that computer concepts. Indeed, with this software, the user can interact with the program via control functions and indicators located in a front panel so-called "user interface". All procedures and controls are defined in a subprogram called "block diagram". This last allows to link the modules used in the user interface and the actions to which they refer. However, this part hides when using the program. It is only useful when programming, changing or adding functions. The user is not necessarily the programmer. The program can be used without having to decrypt the programming.

The second goal is to make the control as friendly as possible. Anybody should be able to use the equipment by just having a quick look of the first page. To help the user a system diagram shows the different parameters involved. It appears on the right of the control panel. This last is composed of four blocks. The first being the button to reset the program and/or to shutdown the whole system. In resetting the system, all parameters are automatically initialized. A dialog box asks the user to enter the borehole length, the borehole radius, the data save time interval and his/her email address. These parameters will be used for analysis or to alert the user in case of any malfunctioning (see after). The second is the block dedicated to start a new test, with a "start-stop" button, a display of the elapsed time and the launching date and time. The third block is used for the activation and setting of the working components, which are the valve, the pump and the heater. The user can operate and adjust the system with these three blocks. However, the programming was done so that no button can be used if the previous one has not been activated or if the system has not reached certain conditions. Indeed, the activation (one after another) of the three working components is only possible after that the initialization is made, and then the test is launched. Once these two conditions meet, the valve can actually be opened. Then, once it is open (positive return set), the pump can be switched on and the flow can be set. Once the flow meter detects the presence of a non-zero flow, the heater can be turned on and the power can be selected. The last block contains all the indicators of temperature (in, out and ambient) and pressure (absolute and differential). On the top of the system diagram, a display of the various events that occur since the beginning of the test was added.

The following figure shows how the interface mentioned above looks like:
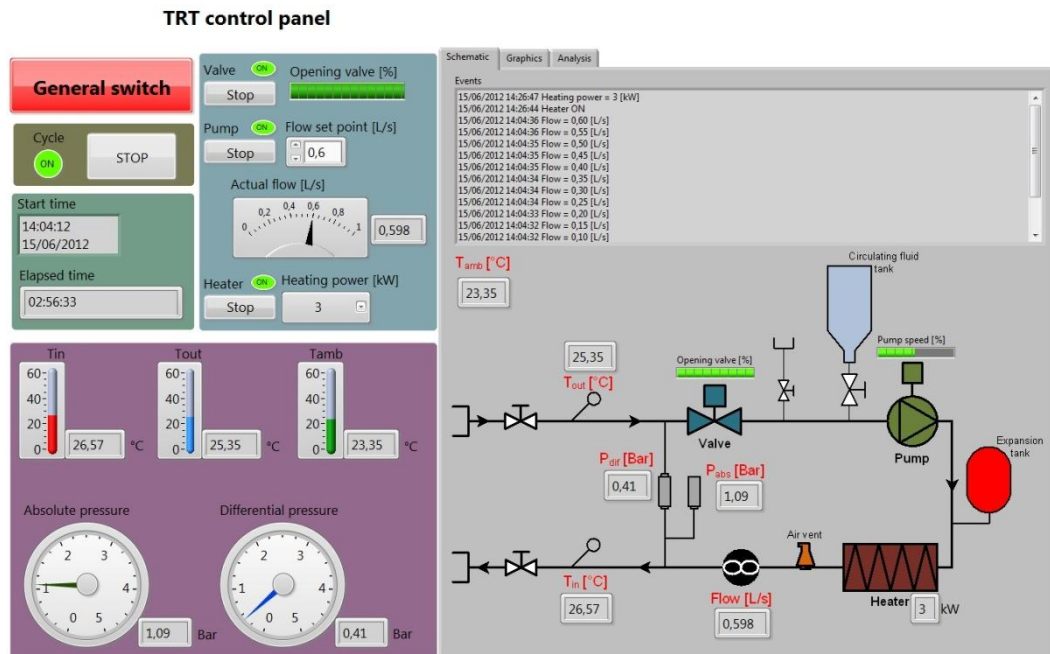
**Figure 16: User interface, "control panel"**

The user has access to this interface via internet. Indeed, thanks to a free software (LogMeIn®) installed on the computer, the user can quickly and easily control the remote computer dedicated to the system via the Internet (as if he/she was sitting in front of it), and this at anytime and anywhere. To run and follow the test, the user has to connect via

the software supplier website (https://secure.logmein.com/). Only a login and a password are necessary. Once the user is logged on his/her account, he/she has to select the remote computer and launch the controlling program installed on the remote computer. Once the user fixed all the parameters, he can log off and let the system run by itself until his/her next connection.

Moreover, in order to make the user interface even more interesting and profitable for the user, additional functionalities have been integrated (*Figure 17* and *Figure 18*). For some of them, the usefulness for the user is indirect. Indeed, preventive and safety alarms have been inserted in the programming code to send email to the user in case of suspicious operating faults and/or to stop the system in case of unwanted conditions. For instance, a too high temperature after the heater, a too high pressure, a quick pressure drop, or a quick flow decrease are watched parameters. These improvements are automatics. However, the user interface offers the option to see the temperature over the time test as well as the thermal injected power and the flow rate evolutions (*Figure 17*). This allows the user to have a better view of the ground behavior, when instantaneous values are not pertinent enough.
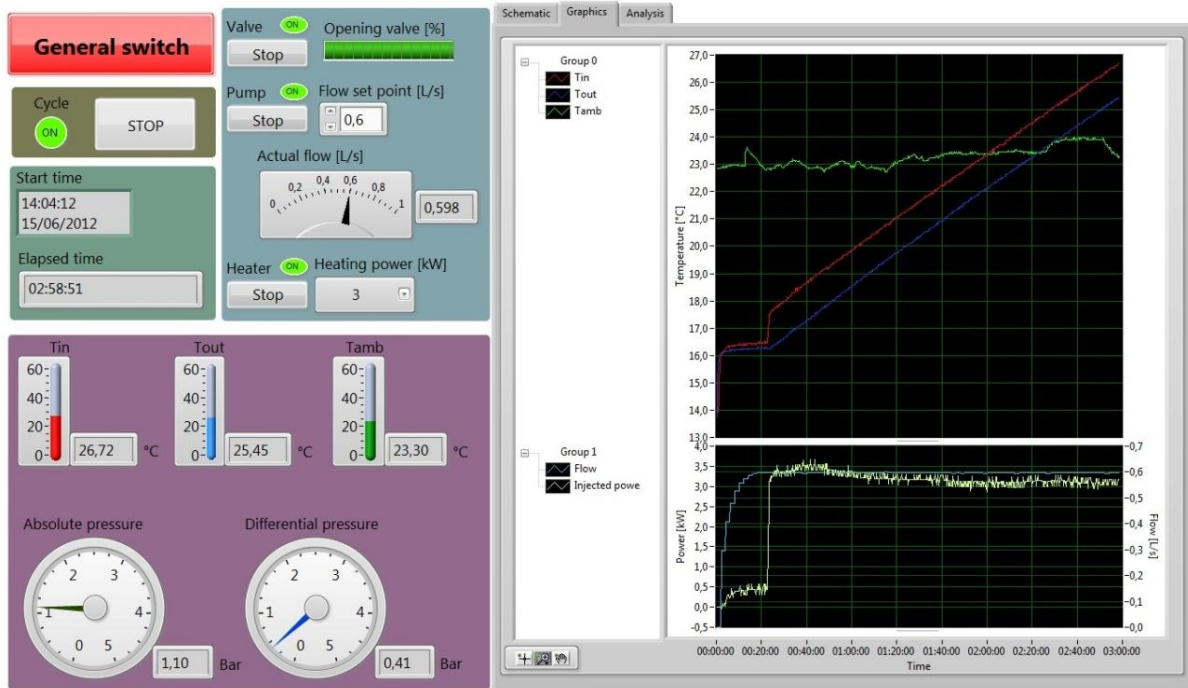
Figure 17: User interface, "graphs"

Moreover, since the idea of a Thermal Response Test is to evaluate the thermal conductivity of the ground and the borehole thermal resistance, a first calculation of these properties is done according to the simplest model presented section 1.3.3.2. The ground undisturbed temperature is also determined even if the user is allowed to change it. Indeed, the ground undisturbed temperature estimation is only correct if the ground is absolutely undisturbed or if was at rest long enough before launching the test. Otherwise, the ground temperature is either higher or lower than the undisturbed temperature due to the use of the BHE or previous thermal response tests, which must be taken into consideration during the TRT analyses.
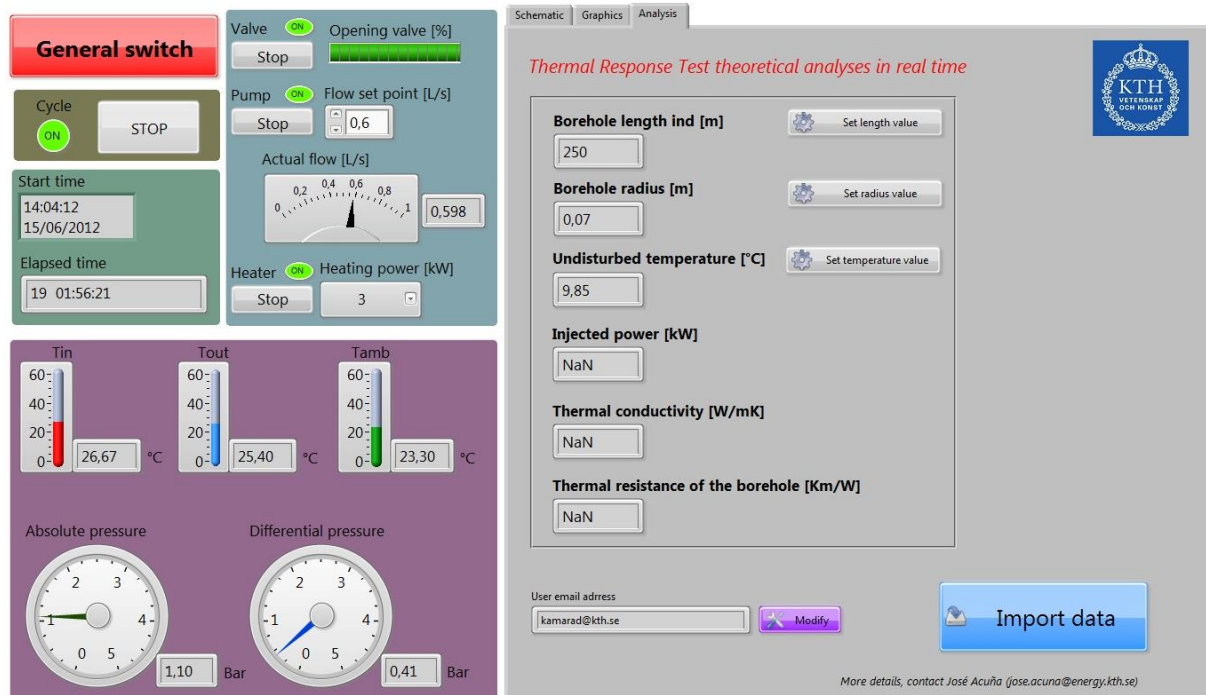
Figure 18: User interface, "analysis"

The theoretical analysis in this program is only an approximation! Indeed, the line source model is based on a linear evolution of the mean temperature over the time. However, as it is possible to see on the *Figure 4: Recording temperature profiles* (Acuña J. 2010), the mean temperature (yellow curve) can be assumed linear only 15h after the beginning of the heat injection. This amount of time is only true for this test, but compared to other tests, "15h" can be consider as the minimum time before reaching a linear temperature evolution. Since the analysis must be done by itself, the thermal conductivity of the ground and the borehole thermal resistance are so evaluated after an arbitrary injection period of 15h.

Finally, all recorded data can be downloaded by clicking on a button and specifying the recipient email address. Indeed, the first analysis proposed above is not as accurate as it could be. Beyond the arbitrary injection period, some parameters of the secondary fluid are considered as constant (density and volumetric heat capacity). Therefore, the user must be able to treat the data from a gross file. By this way, he/she will use the correct parameters and he will get better estimation of the thermal properties of the tested BHE.

3. Test of the apparatus in the Lab at KTH

3.1. Running the system in a water tank

Before running the TRT apparatus in a real borehole installation, it was suitable to test it to be sure that the remote control is functional and the constant heat injection is respected. In order to verify those two features, the equipment was connected to a big water tank (*Figure 19*). Indeed, if no fluid circulates inside the system, activating the pump and the heater will lead to the damage of these or even the whole system. Moreover, in this configuration, the large amount of water allows to slow down the fluid temperature increase. A test can then last a sufficient time in order to collect enough data and get representative results.
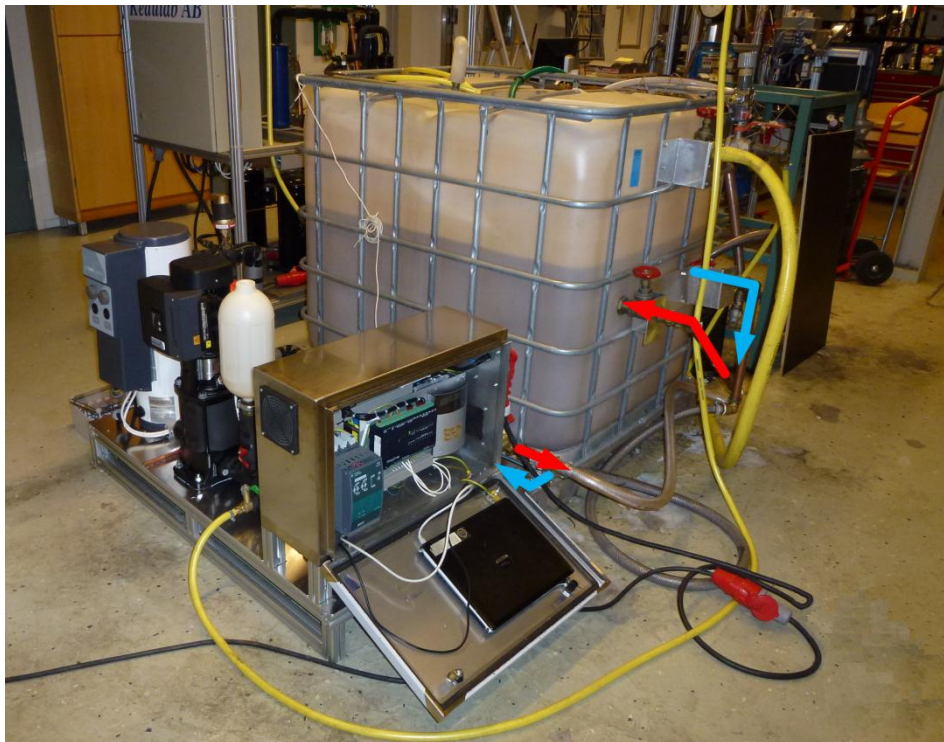
Figure 19: TRT apparatus connected to the water tank

Concerning the remote control system, some modification had to be done. Indeed, as usual when working with controlled devices and system design software, the first use always reveals the programming errors and the improvements that would fit to make the remote control system better. To modify the program (clarity, ease and safety of use) had been quiet fast except for the protocol communication errors between the software and both control units. Indeed, "modbus RTU RS485" and "modbus RTU TCP/IP" are well known communication protocols in automation, but the way to communicate with them depends on the used software. More particularly, the communication is quick and easy when both, the software and the device are from the same company. In the case of this TRT apparatus, the remote control system is composed by independent devices. To understand the protocols and learn how to use the general "module" proposed by software (to ensure writing and reading

between the user and the controlled device) was a long work. However, it was necessary to figure out the error sources and finish the remote control system design. It has been one of the most time consuming problem of the project.

Once the remote control design was validated, the first "real" tests were made. During these tests, as when running the TRT apparatus in a BHE installation, the inlet and outlet temperatures, as well as the ambient temperature, the flow rate and the time are saved. Beyond the temperature profiles over the time, these parameters allow to calculate the thermal heat injected power according to the equation (25):

$$q = \frac{\rho \dot{V} c_p (T_{in} - T_{out})}{2L} \quad (25)$$

With the analysis of this data, it will be then possible to validate (or not) the stabilization of the injected heat power. This study will be presented in the next section.

3.2. Results and discussion

The whole test lasts 4 hours and 20 minutes. The first 40minutes correspond to the flow rate regulation as well as the temperature stabilization in the whole system. Then, for a period of 3h, the heat injection was set to 3kW. Finally, the heat injection and the pump were stopped until the end of the test. During this test, the data was saved every minute. The different temperatures (in, out and ambient) and the calculated thermal power are presented in the following graph:
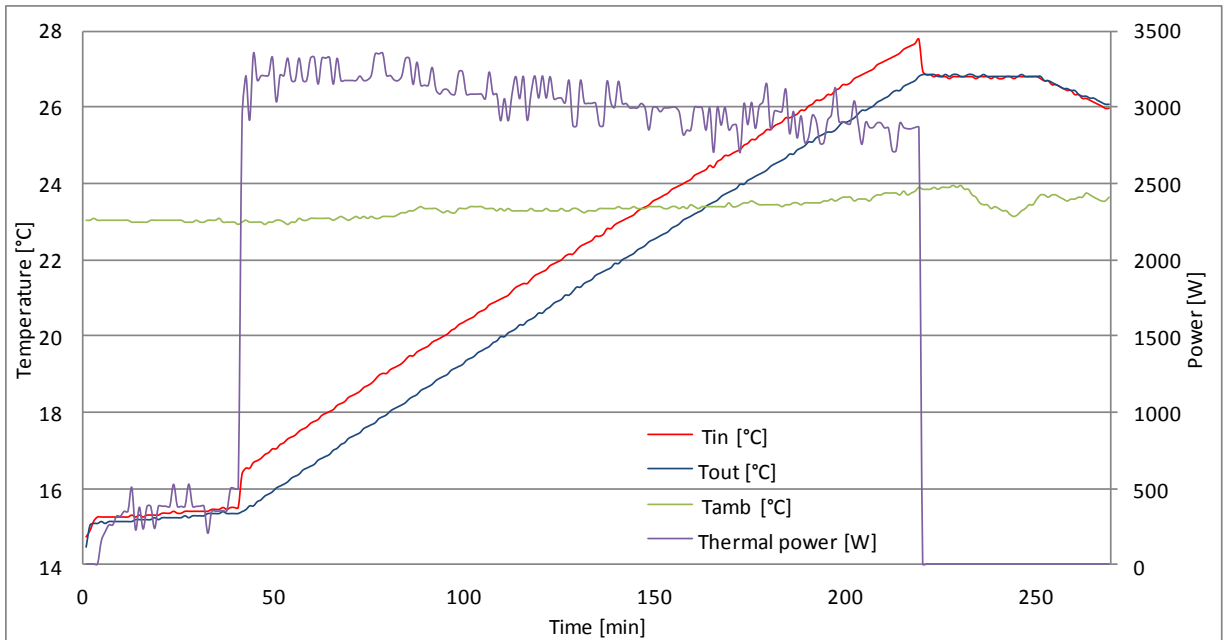
Figure 20: Test of the TRT apparatus with a water tank

The flow rate is plotted in a separate graph since its variations are very small (see *Figure 21*).

First of all, the results highlighted two limits of this test. Indeed, even if the dimension of the water tank is an advantage (as explain section 3.1), such a rig has negative effects. The first

drawback is that the ambient temperature affects the incoming and outgoing temperatures. The ambient temperature change can cause is a redistribution of the heat, i.e. more heat goes to the tank or to the air. The reason is that the tank is open and not isolated. In that case, the heat exchange between the surrounding air and the water inside the tank are favorable, and both in and out temperatures can decrease or increase. The water homogenization in the tank is the second problem. Indeed, no mixing device is installed. The water tank could so have an unwanted "buffer effect" on the water temperature going out of the tank. This could have been solved by letting the test run for a longer time until it reached steady state conditions and it is left as future work if more laboratory tests are going to be done.
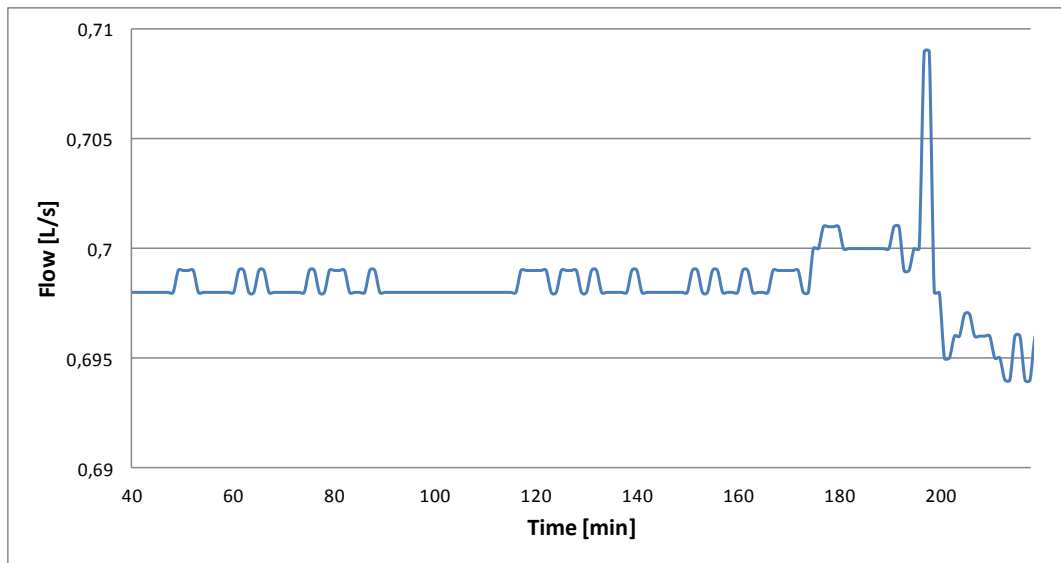
Figure 21: Flow rate during the heat injection

The *Figure 20* does not allow to have precise information on the thermal power injection. The thermal injection is not constant and fluctuates. However, the question is to know how large those fluctuations are. A detailed numerical analysis is so made (see *Table 2*). The study is divided in two parts: the global thermal power analysis and the analysis of the parameters involved in the calculation, respectively.

Table 2: Data analysis of the test with a water tank

	Thermal power [W]		Temperature difference [°C]	Flow [L/s]
	3kW		**3kW**	**3kW**
	The whole injection	From 140 to 170 min	The whole injection	The whole injection
Average	3048,79	2959,81	1,05	0,698
Std deviation	158,47	88,83	0,05	0,002
Error [%]	**5,20**	**3,00**	**5,09**	**0,244**
Max	3357,42	3173,35	1,15	0,709
Min	2705,74	2706,16	0,93	0,694
Diff	651,68	467,19	0,22	0,015
+/-	325,84	233,60	0,11	0,0075
% max-min	**10,69**	**7,89**	**10,51**	**1,074**

Since the power decreases slightly during injection, the thermal power has also been analyzed for a shorter period when the injection was the most stable (from 140 to 170 min). According to standard deviation, the error is between 3 and 5.20%. It is already too high when trying to reach an error of about 1%. These results are confirmed even worst when looking at the "max-min" difference, with 7.89 to 10.69% of error.

The second analysis is tightly linked to the previous observations. Indeed, the thermal power is a function of the temperature difference in and out the system, the flow rate and some additional variables. As shown in *Table 2,* the temperature difference is about 1.05°C and varies with an error of 5.09% during the whole test. The results for the flow are much better with an error of 0.244%. The main source of error in the calculation of the thermal power is then the temperature difference. In contrast, the flow rate can be considered as constant and its error contribution as negligible.

In order to understand the reasons of such temperature measurement errors, the temperature measurement system was verified. Indeed, the resistance sensibility of the DAQ unit is 0.2000 Ω while the PT1000 precision is more or less 3.9 Ω/°C. The global temperature sensibility is 0.0513°C. This value is very close to the standard deviations determined above and explains such errors. Finally, the thermal power fluctuations do not mean that the power in not 100% constant, but only that the temperature measurement system is may not be the best for thermal response test purpose (it is however hard to guarantee better accuracy than ± 0.05K). The idea is so to take a look on the electric part of the heater.

The functioning of the thyristor unit was assumed established and reliable according to the manufacturer recommendations. However, since the results found with calculated thermal power are not exploitable, an analysis of the electric power after the thyristor unit was necessary considered.

Another test, similar to the first one, was then launched in order to get the real electric characteristics supplying the heater. The test is divided in three periods of 30 minutes, each corresponding to a different power load, that is to say: 3kW, 5kW and 9kW. Both, the electric and the thermal powers are monitored. For the electric power, an accurate 3 phase power meter was used (*Yokogawa WT130 Digital Power Meter*). The latter allows to acquire the voltage and the current in each phase and also the total electric power. The evolution of these two powers is presented in *Figure 22.*

The first observation is that the thermal power is always lower than the electric one. Plus, the difference is even more significant for high power loads. This is attributed to "heat losses" which become greater as the power is increase.
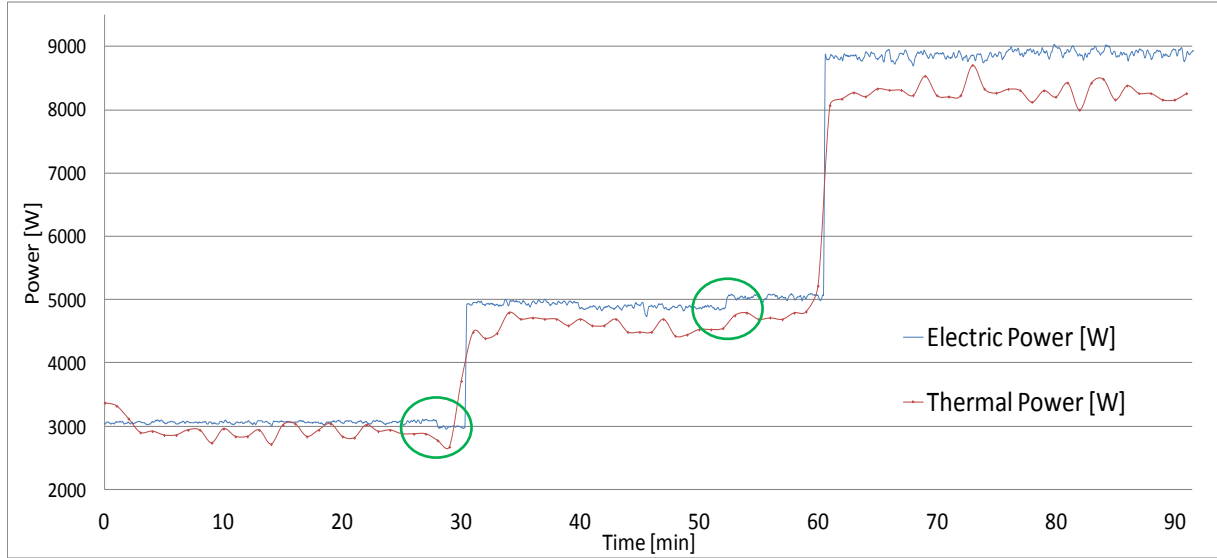
Figure 22: Power after the thyristor (control signal 10V)

However, the thermal power fluctuations are larger than for the electric power. In order to illustrate this observation, three extra figures, one for each heat injection rate, are presented in *Figure 23*, *Figure 24* and *Figure 25*. These three diagrams allow to have a closer view to each part of the test and more clearly observe the fluctuations thanks to a smaller scale (for more details, see in Table 3 and Table 4).
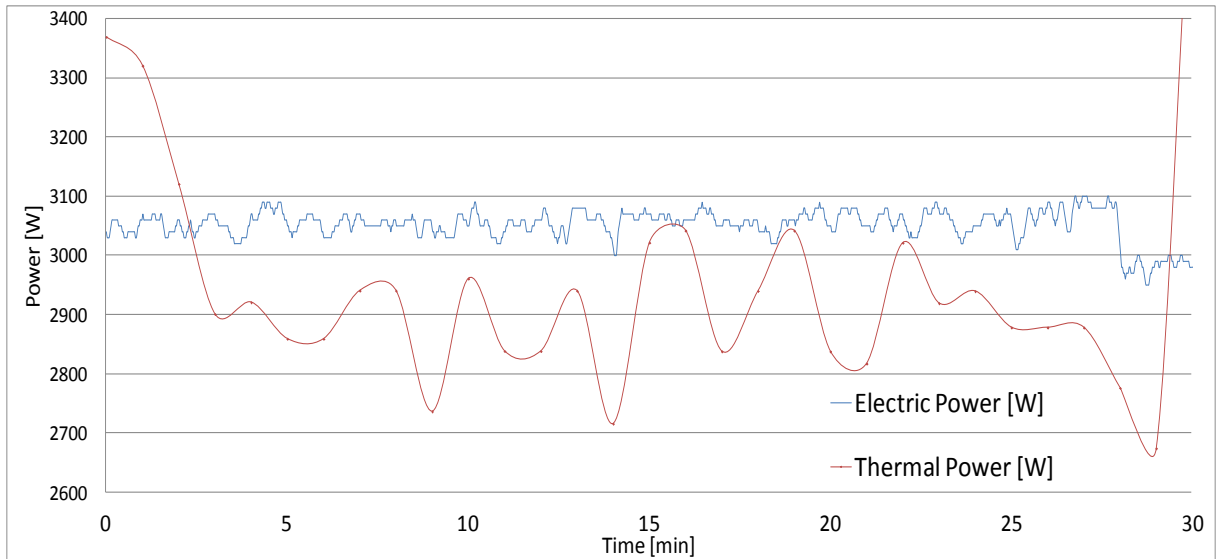
Figure 23: Electric power during the 3kW heat injection
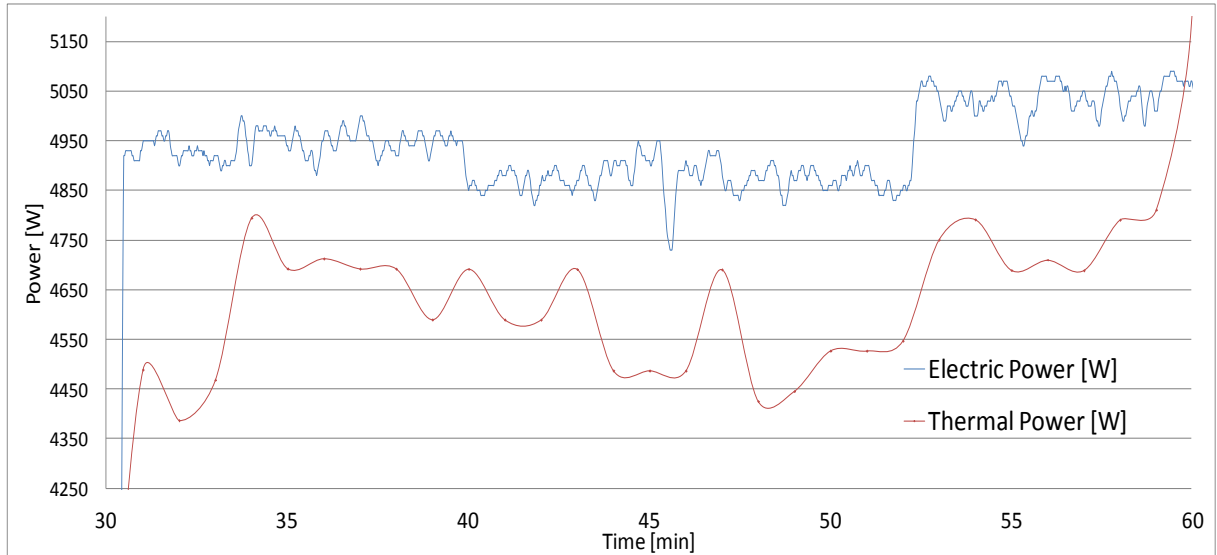
Figure 24: Electric power during the 5kW heat injection
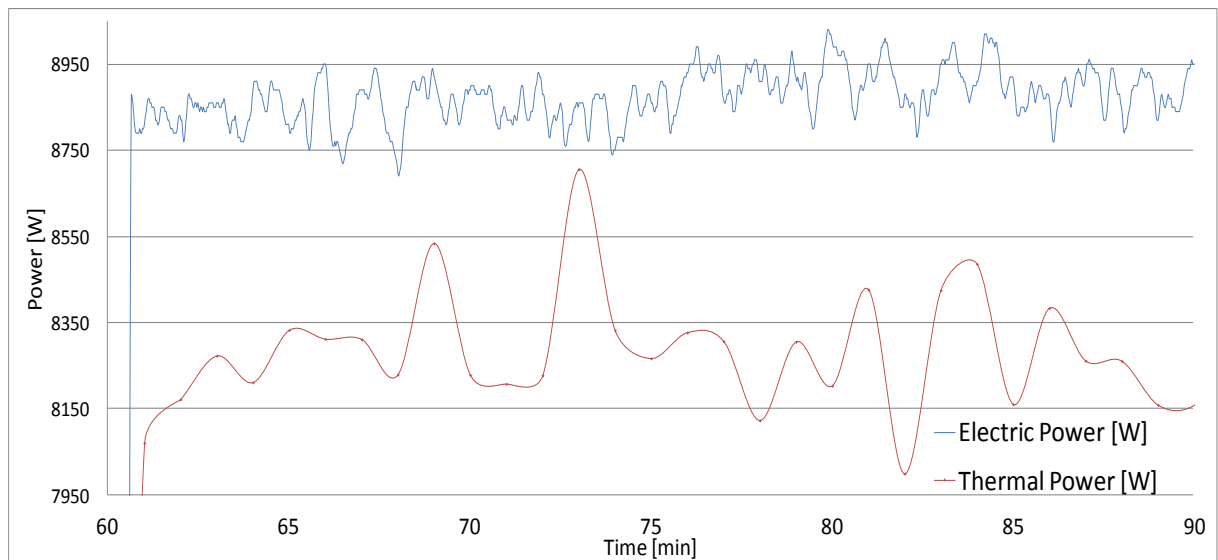
Figure 25: Electric power during the 9kW heat injection

Moreover, as shown the two green circles (see *Figure 22*) when a significant electric power change occurs (during the same power load), the thermal power undergoes the same variation. The calculated thermal power is so well representative of the global power behavior but still not accurate enough. These power changes also point out a problem with the power stabilization since the power is flagrantly not constant. The graph below so emphasizes the fact that the thyristor unit does not work as expected.

To go further in the power stabilization study, the voltage and the current for each phase, as well as the total electric power were analyzed and the results are gathered in *Table 3.*

Table 3: Power analysis from the electric point of view

|	3kW			5kW			9kW		
	V1/ A1	V2/ A2	V3/ A3	V1/ A1	V2/ A2	V3/ A3	V1/ A1	V2/ A2	V3/ A3
	Voltage [V]			Voltage [V]			Voltage [V]		
Average	406,3	407,8	407,9	399,8	401,2	401,4	401,1	402,5	402,8
Std deviation	1,8	1,8	1,8	3,0	2,9	3,0	1,3	1,4	1,3
Error [%]	0,4	0,4	0,4	0,7	0,7	0,7	0,3	0,3	0,3
Max	409,6	411,1	411,1	405,9	407,1	407,5	404,5	406	406,3
Min	399,2	400,8	400,6	391	392,6	392,5	396,9	398,5	398,6
Diff	10,4	10,3	10,5	14,9	14,5	15	7,6	7,5	7,7
+/-	5,2	5,15	5,25	7,45	7,25	7,5	3,8	3,75	3,85
% max-min	1,3	1,3	1,3	1,9	1,8	1,9	0,9	0,9	1,0
	Current [A]			Current [A]			Current [A]		
Average	4,3	4,3	4,3	7,1	7,1	7,1	12,7	12,8	12,7
Std deviation	0,02	0,02	0,02	0,05	0,05	0,05	0,04	0,04	0,04
Error [%]	0,4	0,4	0,4	0,7	0,8	0,7	0,3	0,3	0,3
Max	4,35	4,36	4,36	7,21	7,22	7,21	12,82	12,86	12,84
Min	4,24	4,25	4,25	6,95	6,95	6,95	12,59	12,62	12,6
Diff	0,11	0,11	0,11	0,26	0,27	0,26	0,23	0,24	0,24
+/-	0,055	0,055	0,055	0,13	0,135	0,13	0,115	0,12	0,12
% max-min	1,3	1,3	1,3	1,8	1,9	1,8	0,9	0,9	0,9
	Electric power [W]			Electric power [W]			Electric power [W]		
Average	3051			4940			8875		
Std deviation	26,74			72,47			58,60		
Error [%]	0,88			1,47			0,66		
Max	3100			5090			9030		
Min	2950			4730			8690		
Diff	150			360			340		
+/-	75			180			170		
% max-min	2,46			3,64			1,92		

At first sight, the results seem good. The electric power error is between 0.66 and 1.47 which is quiet small. However, by looking on the "max-min" difference, the results are bigger. This means that there are still some big punctual variations. Moreover, between two different power loads, the error value is never the same or even close. In the worse case, the errors for 5kW are around 50% bigger than for 9kW whatsoever the voltage, the current or the total power. These results unmistakably show that the thyristor unit may be somewhat transparent to the grid fluctuations.

In addition to fluctuations, the voltage varies by step. It is probably due to bigger electric demand changes in the grid. Moreover, the power changes represented by the two green circles (*Figure 22*) correspond to voltage step variations (see the two red marks on the *Figure 26*). This observation could confirm that the thyristor unit does not stabilize the power. However, the grid signal (before the thyristor) must be measured and compared to the signal after the thyristor to make a judgment on its functioning.
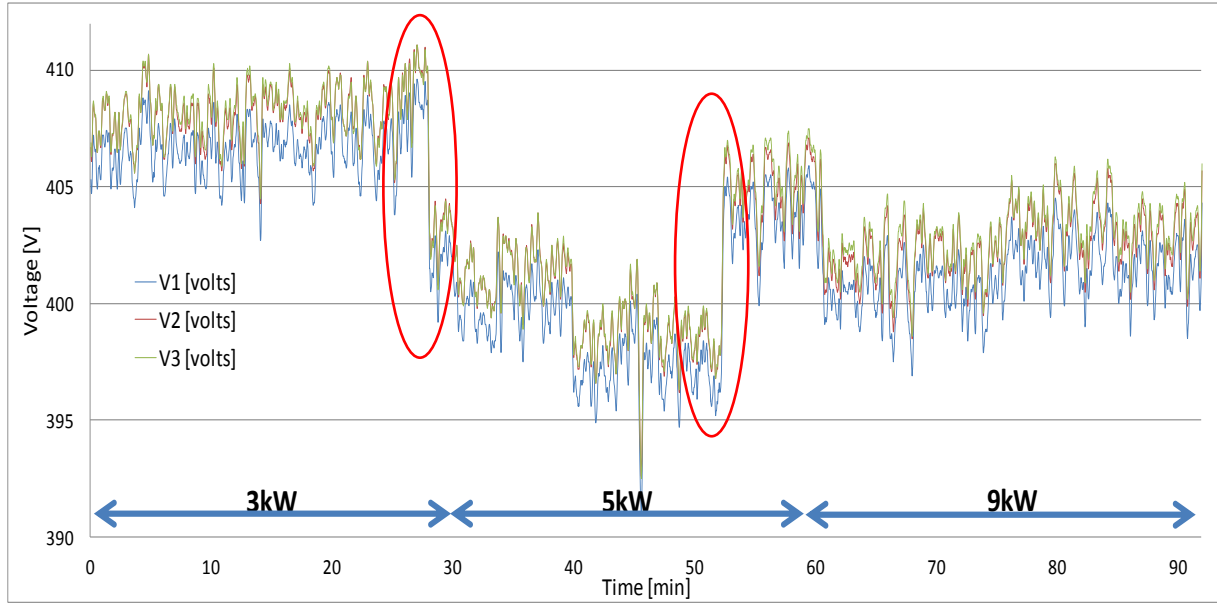
Figure 26: Voltage after the thyristor (control signal 10V)

Finally, a comparative analysis between the electric and the calculated thermal power was made. Once again, the temperature measurement precision distorts the results. Indeed, while the electric power is maximum error for 5kW with 1.47%, the thermal power error is maximum for 3kW with 3.5% and then decreases with the power load increase (see the *Table 4*). The power increases faster than the standard deviation. Indeed, while the standard deviation increases of 33.1% between 3kW and 9kW, the power increases of 186.3%. The standard deviation slightly varies because it depends on the temperature difference error, which is the same for all power loads (around 0.05°C). The thermal power error is so naturally lower for high power load since it is the result of the division between the standard deviation and the mean power.

Table 4: Power analysis from the thermal point of view

	Thermal power [W]		
	3kW	**5kW**	**9kW**
Average	2895,1	4631,9	8289,8
Std deviation	102,7	118,6	136,7
Error [%]	**3,5**	**2,6**	**1,6**
Max	3120,5	4811,1	8706,0
Min	2673,6	4425,4	7998,3
Diff	446,9	385,7	707,7
+/-	223,4	192,8	353,9
% max-min	**7,7**	**4,2**	**4,3**

The calculated thermal power is definitively incorrect and unusable. Regarding the thermal power, no conclusion can be expressed about the power stability.

The last step is to understand the mechanism controlling the thyristor unit. The power going out the thyristor unit (power load) is controlled via an external signal of 0 to 10V. Since the

maximum power supply is 10kW, this signal corresponds to a full scale of 0 to 10kW, and the relation between the control signal and the power load is linear. For instance, in order to get power loads of 3kW and 9kW, control signals of 3V and 9V are necessary.

A last test has been carried out to operate the thyristor unit in several configurations. During this test, the heater was set to 3kW and then 9kW. For each power, the thyristor control signal was arbitrarily modified. Indeed, since the power is not stable when the control signal is set to 10V, the idea is to lower this value and see what happens. The red and blue arrows on the following figure represent the control signal value (in volt) and the heater power, respectively:
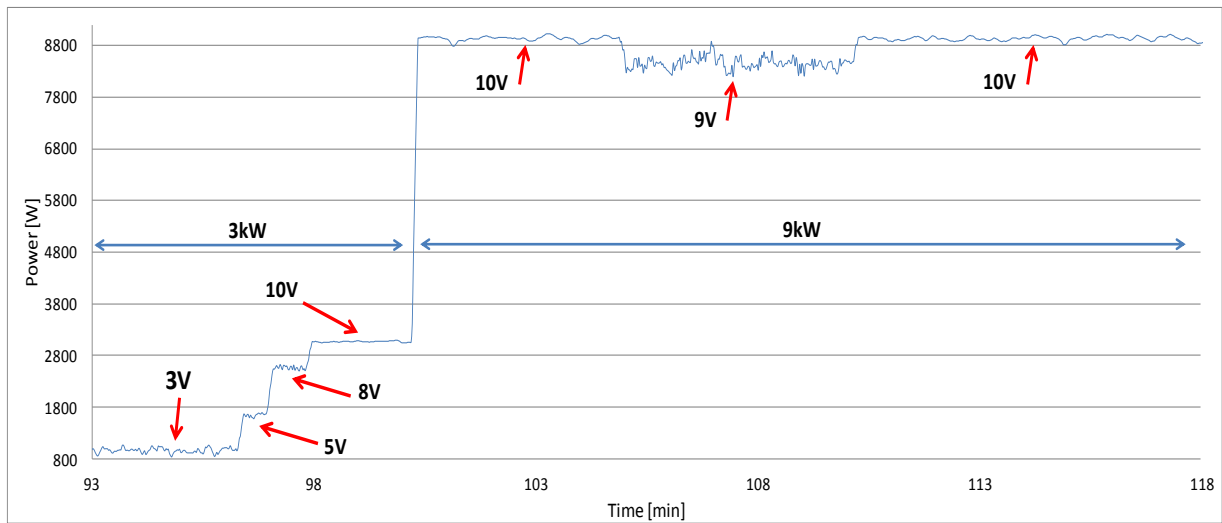
Figure 27: Power after the thyristor for different control signals

According to the control functioning explained above, for 3kW and 9kW, a signal of 3V and 9V would have been perfect. With these settings, the electric power is lower. For 3V and 9V, the electric powers are respectively about 950 and 8450W. These results tally with the control mechanism if the signal conversion corresponds to a full scale of 0kW to the heater power. The thyristor unit then works as a power limiter in which the maximum power is defined by the power of the device.

However, by decreasing the power, the variations increase. Indeed, without analyzing the data, the graph above shows that the fluctuations are much important when the control signal is small (see *Figure 28*).
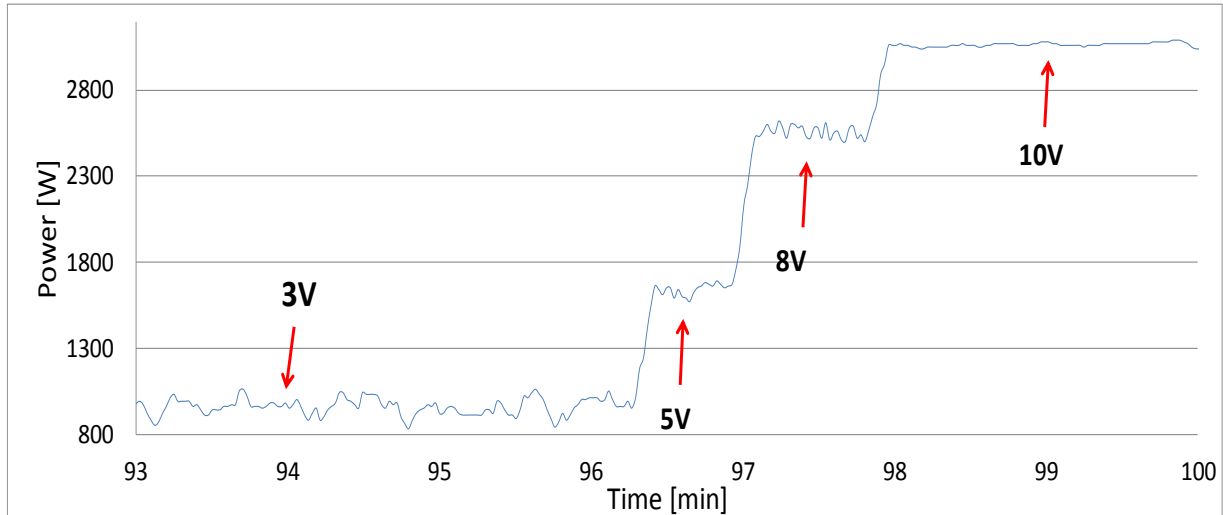
Figure 28: 3kW power load with different control signals

It is right now evident that the thyristor unit does not stabilized the power by itself in an optimum way. The grid fluctuations are very fast and unpredictable. It is so hard to regulate the thyristor unit in real time via the external control signal. Indeed, the period of time between the electric power reading, the regulation, the command sending and the change in the thyristor would be too long compared to the grid fluctuations. It is so very difficult to achieve a continuous regulation with this unit. The regulation must be done inside the stabilization unit.

Despite the fact that the thyristor unit does not ensure an optimum power stabilization, it can be used as an alternative for the power control. Indeed, instead of only three heating power (3, 5 and 9kW), this device would allow to run the equipment from 0kW to 9kW. The only restriction is that the new power stabilization system must be able to compensate for the variations increase for low powers (thyristor control signal lower than 10V).

The conclusion of the whole analysis is the following: The calculated thermal power is not accurate enough and cannot be used to verify the power stabilization. The temperature measurement system has so to be reviewed and corrected. Moreover, the power stabilization does not seem to be achieved to the fullest.

4. Feedbacks

4.1. Problems met during the project

The delivery of all devices and the apparatus construction took more time than expected. The use and the experiments of the equipment were carried out in just one month. Moreover, some of the components were defective or non appropriate. For instance, the actuated valve was not configured for the good power supply and burnt while its first use. Two more weeks were necessary to get a new valve. Plus, the first electric relays which have been chosen (semi-conductor, solid state relays) were not suitable for the heater control. The switching relays order and the delivery took half a week more. Finally, as said before, to solve the problem of communication between LabVIEW® and the controlled devices was long and complicated.

Despite all these problems, the new TRT apparatus works and compared to the old TRT apparatus, it satisfies most of the new technical and functional features.
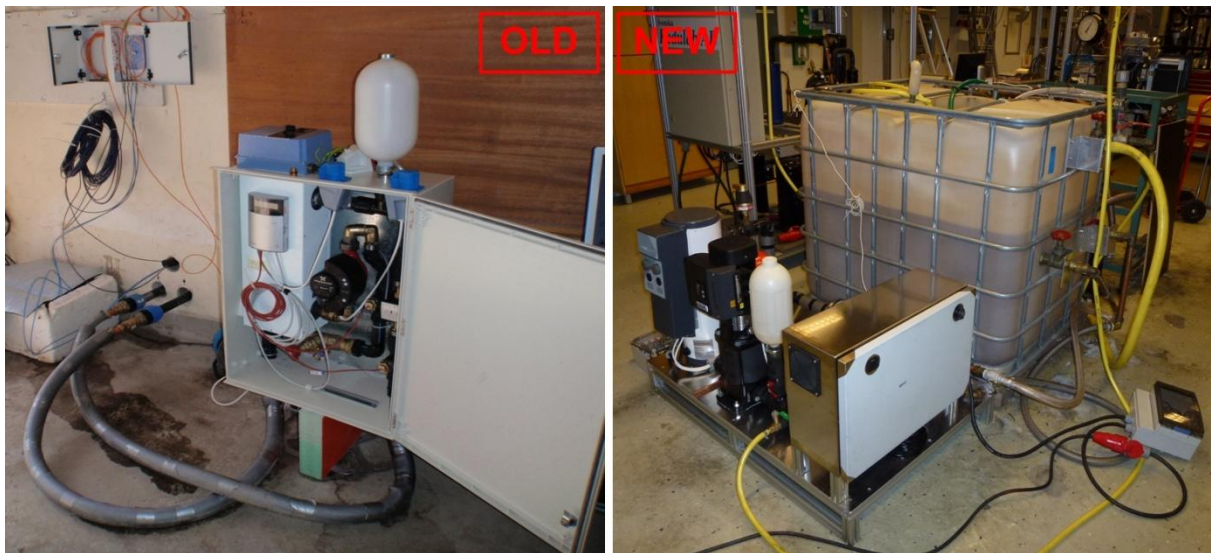

Figure 29: Comparison between the old and the new KTH's TRT apparatus

4.2. Personal experience

In addition to enrich my professional abroad experience, this Master of Science thesis project was the opportunity to go into some knowledge acquired during my studies at INSA of Lyon. It was also the opportunity to tackle important engineer concepts which are not taught at university. Particularly, the constraints in terms of budget and time, or the fact that a study or a project does not necessarily succeed. Communication and teamwork are also two essential parameters that I was able to practice. Last, I developed my personal skills as well as an important autonomy in my work.

5. Conclusion

The design and the construction of this mobile equipment for thermal response test in borehole heat exchangers has been almost achieved. In terms of components, everything works properly. Only the cover has to be added. Finally, the last improvement would be to put the whole system in a trailer for easy transport on hardly accessible sites. The electronic part with the control system (remote) is completed. The equipment can operate and a test can be launched once the system is connected to a borehole. The TRT apparatus is designed "plug and play". Nevertheless, two elements in which an essential must be reconsidered. The temperature measurement system has to be changed for a more accurate one. Last but not least, a new device may need to be found in order to stabilize the power injection. The thyristor unit does unfortunately not seem to fully provide this function. The new TRT apparatus offers, however, larger use possibilities than the old KTH's TRT apparatus.

Future works

The TRT apparatus being not fully completed, the person in charge of the project continuity should:

➢ Re-check and/or find a suitable power stabilizer for the system (compact and efficient);

➢ Study possible ways to get accurate temperature measurements;

➢ Study the possibility of permanently connecting a power meter before and after the stabilization unit and log the electric power loads in order to have two means of control on the heat injection.

6. References

Acuña J. (2010). *Improvements of U-pipe Borehole Heat Exchanger.* Licentiate Thesis in Energy Technology 2010. Stockholm: KTH.

Acuña J. (2008). *Characterization and Temperature Measurement Techniques of Energy Wells for Heat Pumps.* Master of Science Thesis. Stockholm: KTH.

Acuña J, Mogensen P, Palm B (2012). *Distributed Thermal Response Tests on a Multi-pipe Coaxial Borehole Heat Exchanger*, 2011. HVAC&R 17:6, 1012-1029.

Bayer et al. (2012). *Greenhouse gas emission savings of ground source heat pump systems in Europe.* Renewable and Sustainable Energy Reviews. Volume 16, Issue 2, February 2012, Pages 1256–1267.

Berberich, H., N. Fisch, and E. Hahne (1994). *Field experiment with a single duct in water saturated claystone.* Proceedings of 6th International Conference on Thermal Energy Storage, Calorstock '94, August 22-25, 1944, Espoo, Finland.

Carlslaw H.S., J.J.C. (1959). *Conduction of Heat in Solids*, 2d ed Great Britain: Oxford Science Publications.

Choudary A. (1976). *An approach to determine the thermal conductivity and diffusivity of a rock in situ.* PhD thesis, OSU.

Claesson J. and Eskilson P. (1988). *Conductive Heat Extraction to a deep Borehole, Thermal Analysis and Dimensioning Rules.* Energy 13/6, 509-527.

Claesson J, Eftring B, Eskilson P and Hellström, G (1985). *Markvärme, en handbok om termiska analyser.* 3 vol., SCBR T16-18:1985, Stockholm.

Contran Alessio and Monaco Lucio (2011). *KTH Remote Pump Laboratory, Technical Report.* March 2011. Stockholm: KTH

Eklöf C, G.S. (1996). *TED- A Mobile Equipment for Thermal Response Test.* Master Thesis 1996:198 E. Luleå: Luleå University Technology.

Eskilson, P. (1987). *Thermal Analyses of Heat Extraction Boreholes.* Lund, Sweden: Department of Mathematical Physics, Lund Institute of Technology.

EUROBSERV'ER (2011). *Baromètre pompes à chaleur.* SYSTÈMES SOLAIRES le journal des énergies renouvelables N° 205 – 2011.

Gehlin Signhild (2002), *Thermal Response Test, Method Development and Evaluation.* Doctoral Thesis. Luleå University Technology 2002.

Gehlin S., Hellström G. (2003). *Comparaison of Four Models for Thermal Response Test Evaluation.* ASHRAE Transaction 2003, Vol 109, Pt. 1.

Gehlin S., Nordell B. (2003). *Determining Undistributed Ground Temperature for Thermal Response Test.* ASHRAE Transactions 2003, Vol 109, Pt. 1.

Gehlin S., Spitler J. D. (2002). *Thermal Repsonse Test – State of the Art 2001.* Report IEA ECES Annex13.

Hellström, G. (1997). *Thermal response test of a heat store in clay.* Linköping, Sweden. Proc. Megastock '97, 115-120.

Hellström G. (1991). *Ground Heat Storage, Thermal Analysis of Duct Storage Systems.* I. Theory. 262 p., LTH.

Ingersoll L.R., P.H (1948). *Theory of the Ground Pipe Heat Source for the Heat Pump.* ASHVE Transactions, Vol.54.

Acuña J and Palm B (2012). *Distributed Thermal Response Tests on Pipe-in-pipe Borehole Heat Exchangers.* Innostock 2012. The 12th International Conference on Energy Storage.

Melinder, Å. (2007). *Thermophysical Properties of Aqueous Solutions Used as Secondary Working Fluids [Doctoral Thesis].* Stockholm: The Royal Institute of Technology KTH.

Mogensen P (1983). *Fluid to Duct Wall Heat Transfer in Duct System Heat Storages.* The international Conference on Subsurface Heat Storage in Theory and Practice, (ss.[Appendix, Part II, p.652-657]). Stockholm.

Monzó P. (2011). *Comparison of different Line Source Model approaches for analysis of Thermal Response Test in a U-pipe Borehole Heat Exchanger.* Master of Science Thesis EGI 2011-017 MSC. Stockholm: KTH.

Reuß et al. (2006). *IEA ECES -ANNEX 21 – THERMAL RESPONSE TEST.* June 2006.

Sanner et al. (2005). *Thermal Response Test – Current Status and World-Wide Application.* Proceedings World Geothermal Congress 2005. Antalya, Turkey, 24-29 April 2005.

http://www.thermalresponsetest.org/